International Journal of Geosciences, 2023, 14, 733-766
https://www.scirp.org/journal/ijg
ISSN Online: 2156-8367
ISSN Print: 2156-8359

Petrography, Geochemistry and Relative Chronology of Quaternary Volcanic Formations in the Mermoz and Fann Sectors, West Senegal

Moussa Fall[1], Ibrahima Labou[2], Papa Moussa Ndiaye[1]

[1]Department of Geology, Faculty of Science and Technology, Cheikh Anta Diop University, Dakar, Senegal
[2]National Superior School of Mines and Geology, Cheikh Anta Diop University, Dakar, Senegal
Email: moussa27.fall@ucad.edu.sn

How to cite this paper: Fall, M., Labou, I. and Ndiaye, P.M. (2023) Petrography, Geochemistry and Relative Chronology of Quaternary Volcanic Formations in the Mermoz and Fann Sectors, West Senegal. *International Journal of Geosciences*, **14**, 733-766.
https://doi.org/10.4236/ijg.2023.148040

Received: July 13, 2023
Accepted: August 27, 2023
Published: August 30, 2023

Abstract

Detailed work on Quaternary volcanism has been carried out in the Mermoz and Fann sectors of western Senegal. In the Mermoz sector, the main emission zone is a collapsed crater located at the intersection of three major fractures: NE-SW, NW-SE and N-S. The lithological succession in this Mermoz sector comprises, from bottom to top: 1) a substratum with at its base Eocene limestones on which lie Quaternary sands surmounted by stratified tuffs; 2) a vesicular ball dolerite which deforms the stratified tuffs; 3) a dark early breccia; 4) two generations of basanites: the first is vesicular, the second non-vesicular; 5) a clear intermediate breccia and finally 6) a late breccia. The Fann sector contains several emission zones, most of which are currently located in the ocean. The lavas may have reached the coast through E-W and NE-SW faults. The lithological succession includes from bottom to top: 1) scoria-rich early volcanic breccias; 2) a first generation of non-vesicular mesocrate dolerite (D1); 3) a second generation of melanocrate vesicular dolerite (D2); 4) basanites and finally 5) a late breccia. The geochemical characteristics of the lavas studied are compatible with a very enriched and very deep magmatic source of the garnet lherzolite type located in the lower mantle. The magma from this source would have risen in the form of mantle plumes through major NE-SW and E-W faults in a continental intraplate context.

Keywords

Quaternary Volcanism, Western Senegal, Emission Zone, Geochemistry, Continental Intraplate

1. Introduction

The west extremity of Senegal (Figure 1) was, at the end of the Tertiary (Miocene)

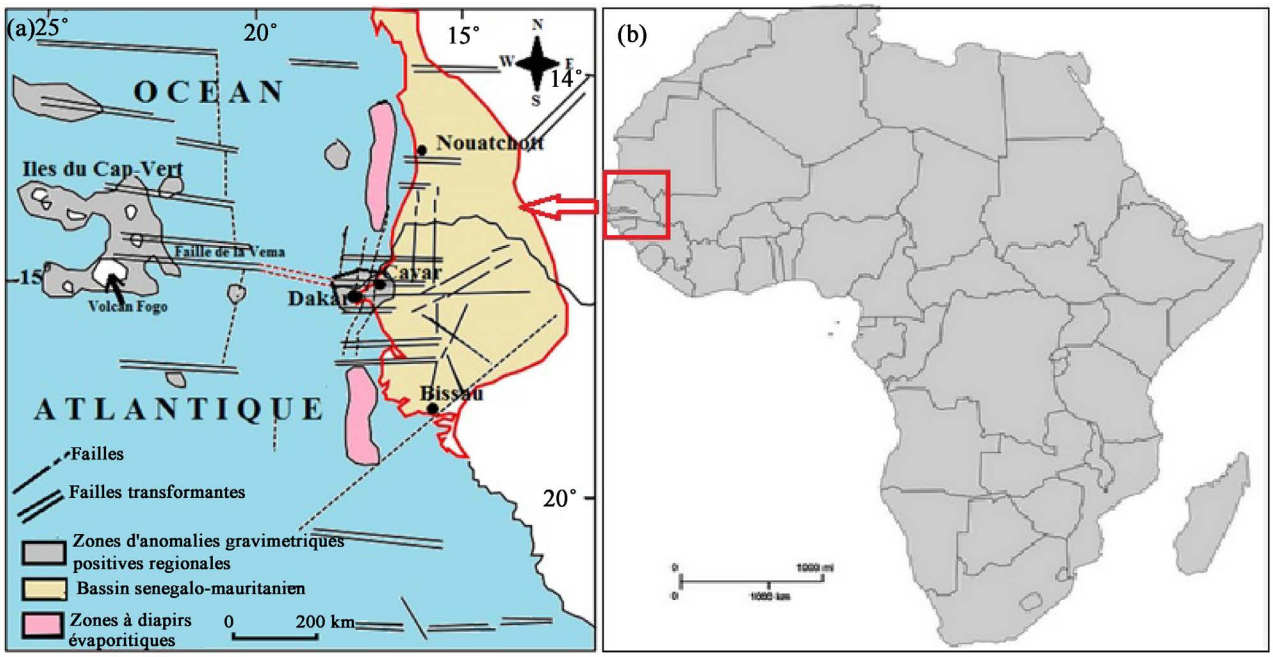

Figure 1. Location maps: (a) Location map of the West African continental margin (after [2]). (b) Location of Senegal on the map of Africa.

and at the beginning of the Quaternary, the seat of an important basic magmatism. This magmatism is closely related to the N-S oriented brittle tectonics whose manifestations, are linked to the opening of the Atlantic [1].

Previous studies ([3]-[18]) have mapped Tertiary and quaternary volcanism and provided insights into emplacement modes.

Quaternary magmatism, the subject of this article, outcrops only in the Dakar region, in its northwestern part, and is represented by two craters: a main crater located at Mamelles and another secondary located at Mermoz ([6] [13] [16] [19]).

However, these authors also suggested the existence of other exit points at "Toundis", at the tip of Almadies-Yoff and at Fann, but no research has been carried out to confirm or refute this hypothesis.

Thus, the aim of this article is to study in detail the sectors of Mermoz-Plage de Fann résidence (Mermoz sector) and Place du Souvenir-Université (Fann sector) in order to characterize the different volcanic formations, establish a relative chronology and highlight a secondary exit point at Fann.

In addition, new geochemical data have been implemented in the two sectors to better characterize origin of the magmas and to propose a geotectonic context.

2. Geological Context

The west part of the Senegalese-Mauritanian basin has known during geological history, three major periods of volcanic activity:

- The first period, from the Upper Cretaceous to the Paleocene, is recognized by drilling [20]. It is represented by hornfels with enclaves of microsyenits of the Léona dome, trochoid tuffs in the Dakar region. The Léona dome was set up at

the beginning of the Maastrichtian [2]. The trochoid tuffs would come from probably submarine volcanic projections.

- The second period of the Tertiary age is represented by around thirty volcanic bodies, most often small in size, and at depth by numerous vein bodies encountered in wells and boreholes ([2] [3] [10] [21]). There are no longer any parts of well-preserved aerial apparatus, and numerous outcrops in fact correspond to ancient sub-surface intrusions. About ten diatremes and numerous sills and tuff dykes have been recognized [22]. Witnesses of Tertiary volcanism fall into four geographical groups (**Figure 2(a)**):

- Dakar system, where the most extensive basaltic outcrops that may correspond to flows are found (Cap Manuel, Gorée, Madeleine Islands);
- Rufisque unit, where tuffs are abundant;
- Ndiass dome unit, which includes many small lava and tuff intrusions, linked to faults;
- Thiès region unit, where the main outcrop, that of Diack, probably corresponds to the remains of a lava lake established in a maar [16].

- The third period is of the Quaternary age and is located only in the head of the Cap-Vert peninsula (**Figure 2(b)**). This period gave birth to the Mamelles volcano which is a polygenic device built over several phases of activity of different dynamism. It shows successively:

- The oldest known episode of the Mamelles: it is a basalt flow whose top is particularly coarse; which gives it a doleritic appearance macroscopically;
- The Strombolian episode whose products are tuffs and cinerites, surmounted

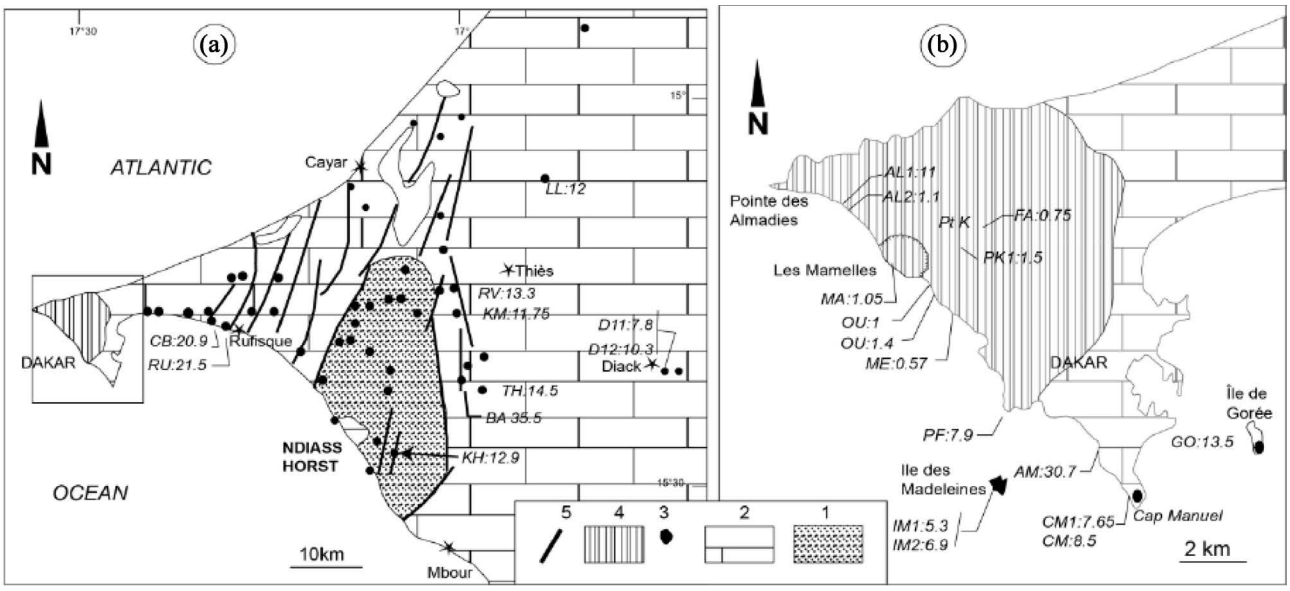

Figure 2. Location map of volcanism on the Cap-Vert peninsula and Thiès (after [16]). (a): Cape Verde peninsula and Thiès region. (b): Head of the Cape Verde peninsula containing the study zone. 1: Secondary; 2: Tertiary carbonate; 3: Tertiary volcanic outcrops; 4: Quaternary volcanic outcrops; 5: Faults; CB: Cap des biches; RU: Rufisque; LL: Lam-lam; SS: Sène Sérère; D: Diack; RV: Ravin des voleurs; TH: Thiéo; BA: Bandia; KH: Khazabe; AL: Almadies; MA: Mamelles; OU: Ouakam; ME: Mermoz; FA: Fort A; PK: Point K; PF: Pointe de Fann; AM: Anse des Madeleines; IM: Ile des Madeleines; CM: Cap Manuel; GO: Gorée. Figure (b) is an enlargement of the framed area in figure (a). The figures represent ages in millions of years.

by slag, and a flow of fine olivine basalt. The highly explosive emplacement is linked to a phreatomagmatic phenomenon [7];

- The Hawaiian episode is the most widespread surface flow in the Quaternary and covers more than 80 km^2. It consists of a very fluid flow whose top tends to be doleritic, but which gradually passes to a microlitic base loaded with olivine.

Other secondary emission points have also been highlighted: Doleritic veins at the tip of Almadies and the chimney of Mermoz in Fann, which intersects several flows from the Mamelles volcano ([6] [19]).

3. Materials and Working Method

Several field trips during low tides were carried out on the basis of available maps and geological sections. The works carried out on outcrops of excellent quality consisted of identifying the different lithologies, analyzing the geometric relationships between facies in order to define a relative chronology, making macroscopic petrographic descriptions of the samples, making structural measurements and finally taking samples for making thin sections and for geochemical analyses. The microscopic petrographic studies were made using a microscope equipped with a camera at the Department of Geology and at the Fundamental Institute of Black Africa (IFAN) of Cheikh Anta Diop University of Dakar (Senegal). Analyzes of major and trace elements on whole rocks were carried out in Canada by the ACTLABS laboratory (Laboratory No.A21-02232). The major elements were analyzed by the FUS-ICP method and the trace elements by the FUS-ICP and FUS-MS methods.

4. Results

4.1. Lithology and Petrography

4.1.1. Mermoz Sector

The geometrical and chronological relationships between the different formations of the Mermoz sector show from bottom to top: 1: marly limestone; 2: infra-basaltic sands; 3: bedded tuffs; 4: balled dolerite; 5: scoriaceous polygenic breccia; 6: basanites; 7: clear polygenic breccia rich in volcanic bombs and clayey cement and 8: late breccia most often monogenic.

- **Marl limestones**

These rocks (**Figure 3(a)**) outcropping at the northern end of the "Water front" hotel mark the end of the Tertiary. They underwent thermal metamorphism in contact with a dolerite intrusion. They are also observed as enclaves in dolerites and basanites.

- **Infra-basaltic sands**

About 5m thick (**Figures 3(a)-(c)**), these sands dating from the Quaternary [23] overlie the marly limestone. The contact between these two formations is highlighted for the first time in the west coast of Dakar. Infra-basaltic sands are a typical formation of a high-energy littoral environment [23].

Figure 3. Lithology and petrography of the Mermoz sector: (a) tertiary limestone (Cal.) at marly levels covered by infra-basaltic sands (San.), all intersected by a dolerite intrusion; (b) intrusive ball dolerite in an assemblage consisting of infra-basaltic sands (bottom) and stratified cineritic tuffs; the stratification plan of the tuffs are deformed by the intrusion. (c) covered infra-basaltic sands and cinerites, cut by a basanite flow (Bas.); (d) texture of balled dolerite showing strongly weathered pyroxene (Px) phenocrysts and plagioclase (Pl) and (e) and (f) basanite in sill in the breccia (Br.).

- **Bedded tuffs**

These are cinerites, which outcrop along the coast (**Figure 3(b)**, **Figure 3(c)**) on either side of the volcanic apparatus of Mermoz and around the Radisson hotel. These rocks top the infra-basaltic sands and show well-stratified levels with alternating clear beds and brown beds. They are made up of small elements joined together by very fine cement, with a sedimentary appearance. To the north of the Water Front hotel, the tuffs show intersecting stratifications in their upper part. These cinerites are sometimes reddened and their thickness decreases towards the south.

- **Dolerite in balls**

The dolerite of the Mermoz volcano is cut into balls of various sizes that can exceed 3 m in diameter. The best outcrops are located near the "Mermoz swimming pool" and north of the Water Front Hotel (**Figures 3(a)-(c)**). Other outcrops are located in the cove of Ouakam. [16] locates this dolerite under the infra-basaltic sands. They dated it at 1.4 ± 2 Ma and named it a medium volcanic unit, which would correspond to a single flow having undergone lateritic alteration before its burial under the infra-basaltic sands. Our new observations do not militate in favor of this conclusion. Indeed, we noted that the dolerite in balls intersects the Tertiary carbonate formations, the infra-basaltic sands and the stratified tuffs. The bedding planes of these tuffs have been uplifted and deformed by dolerite into balls (**Figure 3(b)**). This dolerite contains enclaves of metamorphosed sedimentary rocks. It is observed itself in the form of an enclave in the basanites of the Mermoz volcano. Under the microscope, the balled dolerite shows an intergranular doleritic texture marked by contiguous laths of plagioclase what create spaces occupied by pyroxenes (**Figure 3(d)**). Plagioclases are present inmacrocrystals and microcrystals. Plagioclase macrocrystals show clear polysynthetic twins. Interstitial pyroxenes also occur in macrocrystals and microcrystals. Less abundant pyroxene macrocrystals are automorphic to sub-automorphic and sometimes altered to opaque minerals.

- **The scoriaceous breccia**

The scoriaceous breccia forms a thick layer marked by a very advanced alteration, which gives it a characteristic red color. It consists of fragments of scoria and large-grained dolerite (dolerite in balls). The explosions at the origin of the scoriaceous breccia preceded the placement of the basanites. Indeed, the breccia is cut by numerous basanite dykes and sills (**Figure 3(e)**, **Figure 3(f)**).

- **Basanites**

They were set up from several exit points that are difficult to highlight. Some of these emission points are located in the ocean and the lava could only reach the mainland through fractures, especially those oriented NE-SW and E-W. At the level of the Mermoz volcano, at least two generations of basanites have been clearly identified (**Figure 4(a)**, **Figure 4(b)**). The basanites cut the dolerite in balls, the infra-basaltic sands and the stratitified tuffs. These tuffs come from the Mamelles volcanic apparatus. The first generation of basanite (basanite1) is vesicular and cut into vertical prisms and elongated slabs. The main outcrop of this

Figure 4. Lithology of the Mermoz sector (continued): (a) massive basanite 2 (Mas. bas) in sill in bullous basanite 1 (Bul. bas); (b) massive basanite 2 (Mas. bas) as a dyke in bullous basanite 1 (Bul. bas); (c) enclave of peridotite (Per.) in massive basanite; (d) and (e) enclave of dolerite in massive basanite and (f) volcanic bomb in massive basanite.

basanite is located in the western part of the Mermoz volcano and continues into the ocean in a NE-SW direction.

The second generation of basanite outcrops in the eastern part of the Mermoz volcano where it is oriented NE-SW. This second generation of basanite (basanite2) is globally non-vesicular. It is presented in vertical prisms whose

superficial parts are fractured and cut into horizontal plates. In the western part of the volcano, the second basanite can be injected in the form of veins and sills into the first basanite (**Figure 4(a)**, **Figure 4(b)**) and into the tuffs. Basanites may contain enclaves of peridotites (**Figure 4(c)**) dolerites (**Figure 4(d)**) volcanic bombs (**Figure 4(e)**) and cinerite (**Figure 4(f)**). Microscopic observation of the vesicular basanite shows a porphyritic microlithic texture (**Figure 5(a)**).The mineralogical composition consists of a primary paragenesis with plagioclase, pyroxene and olivine and a secondary paragenesis with opaque minerals. Plagioclases form microlites that define a discrete planar orientation. Pyroxenes occur in microlites. Olivine occurs in phenocrystals and microcrystals. Olivine phenocrysts are automorphic to sub-automorphic and sometimes completely altered to iddingsite (**Figure 5(a)**). Microscopic observation of the massive basanite shows the same texture and the same mineralogical composition as the vesicular one. The minerals of this basanite are little altered and show no gaps (**Figure 5(b)**).

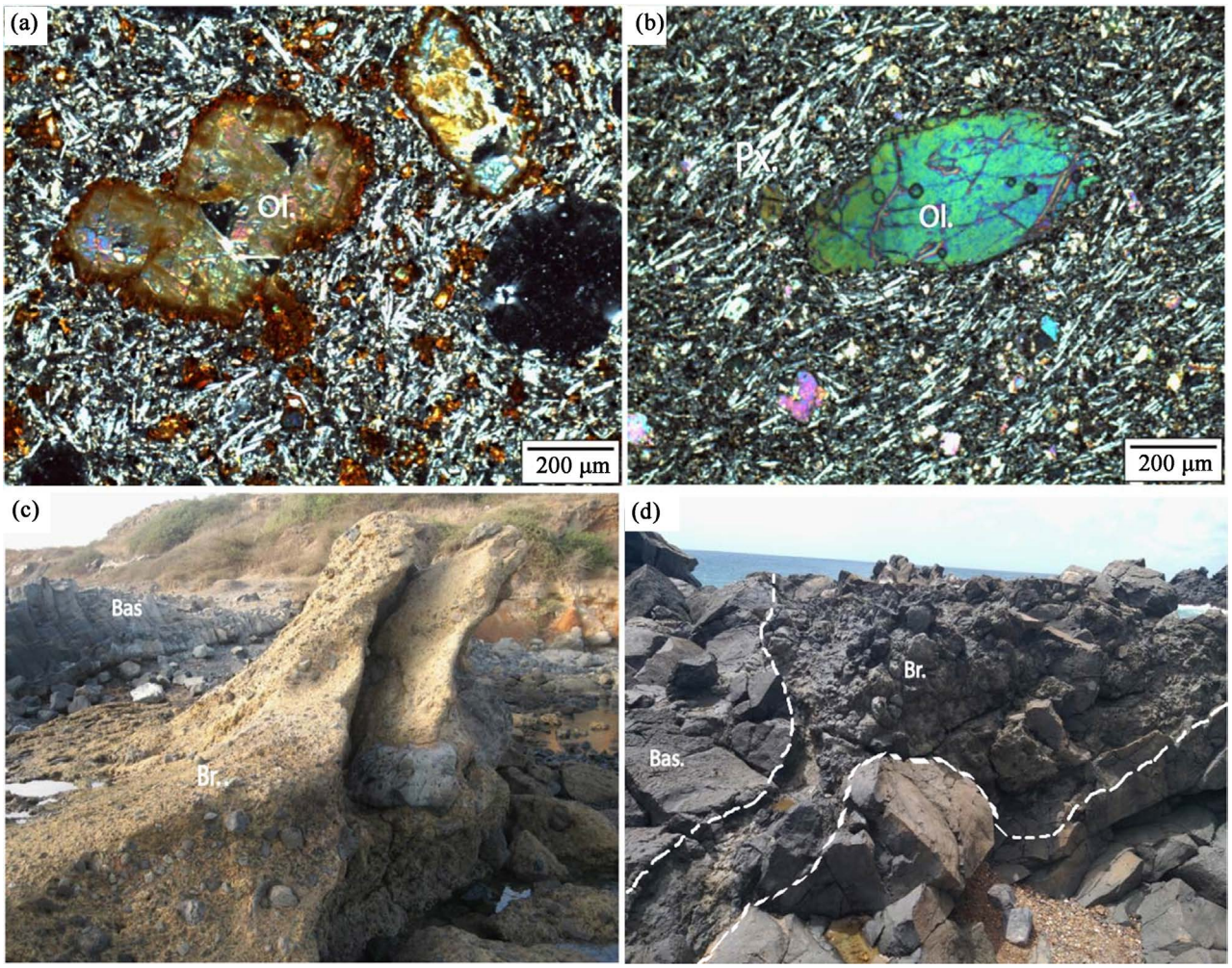

Figure 5. Lithology and petrography of the Mermoz sector: (a) porphyritic microlithic texture of vesicular basanite; (b) porphyritic microlithic texture of massive basanite; (c) clear breccia in contact with massive basanite cut into prisms slightly dipping to the SW and (d) breccia resulting from a late explosion within the massive basanite according to N140 fractures.

- **The clear breccia with clay cement**

This breccia mainly outcrops in the eastern part of the Mermoz volcano in the form of a small mound about 4 m high (**Figure 5(c)**).These breccias are the result of phreatic explosions and are located at the limit of the stratified tuffs of the Mamelles volcano. Clay cement gives it a characteristic beige color. This cement brings together various elements whose size can reach 120 cm. Among these elements, we distinguish coarse-grained dolerites, vesicular basanites, massive basanites and basaltic slags. The breccia cuts very clearly the infra-basaltic sands and the stratified tuffs. On the other hand, its chronological relations with the basanite2 with which it is in contact are not very clear. But we can think that the inclination of this basanite towards the SW was caused by the explosions at the origin of the breccia. This interpretation is supported by the presence in the breccia of basanite elements whose prismatic flow resembles that presented by basanite 2.

- **The late breccia**

It represents the ultimate manifestation of the Mermoz volcano. The explosions occurred within the basanites themselves along fractures N140 (**Figure 5(d)**) and N50. The breccia is generally monogenic and essentially consists of basanite fragments joined by tuffaceous cement. However, there are small fragments of coarse-grained dolerite in places.

4.1.2. Fann Sector (Remembrance Square-IFAN Cheikh Anta DIOP)

All the formations outcropping in this sector, which show from bottom to top: stratified tuffs, an early volcanic breccia, and dolerites belonging to two generations (D1 then D2), basanites and finally a late volcanic breccia.

- **Stratified tuffs**

These tuffs outcrop a few meters away, at the height of the Embassy of Mali (**Figure 6(a)**). They show stratification with clear beds about 30 cm thick. The strata show alternating yellow to pinkish very fine grained beds. These tuffs are cut by doleritesills.

- **Scoriaceous breccias**

These breccias outcrop at the "Place du Souvenir" (**Figure 6(b)**). They are monogenic essentially made up of slag elements united by clay cement corresponding to the pulverized substratum (infra-basaltic sands and stratified tuffs). The slag elements are generally angular and their size varies between 5 and 15 cm. The volcanic breccias are cut by dolerite and basanite veins. Microscopic observation of the slag fragments reveals a porphyritic microlithic texture with olivine phenocrysts (**Figure 6(c)**). The primary paragenesis consists of plagioclases, olivines and pyroxenes. The sometimes zoned olivine phenocrysts are very often altered to iddingsite, which forms reddish spots.

- **Dolerites**

They outcrop along the coast, between the "Place du Souvenir" and the Hotel Térou-bi. Two generations of dolerites have been observed. The first named D1 is omnipresent and sometimes extends inside the ocean thus constituting points

Figure 6. Lithology and petrography of the Fann sector: (a) layered tuff cut by D2; (b) monogenic volcanic breccia; (c) texture of an element of the monogenic breccia (MF300); (d) D1 dolerite cut into vertical prisms and (e) D2 dolerite into veins and stringers in D1.

like the one in front of the residence of the Embassy of Mali. Dolerite D1 shows a lower part cut into a prism (**Figure 6(d)**) and a superficial part altered into a ball. She is often affected by numerous fractures. Very rarely vesicular, D1 dolerite always shows a micrograined texture with a medium grain and a light gray appearance which contrasts with the melanocratic aspect of the second generation of Dolerite (D2) which is vesicular everywhere. This D2 dolerite intersects D1 in the form of tubes (**Figure 6(e)**), veins (**Figure 7(a)**), stringers (**Figure 7(b)**)

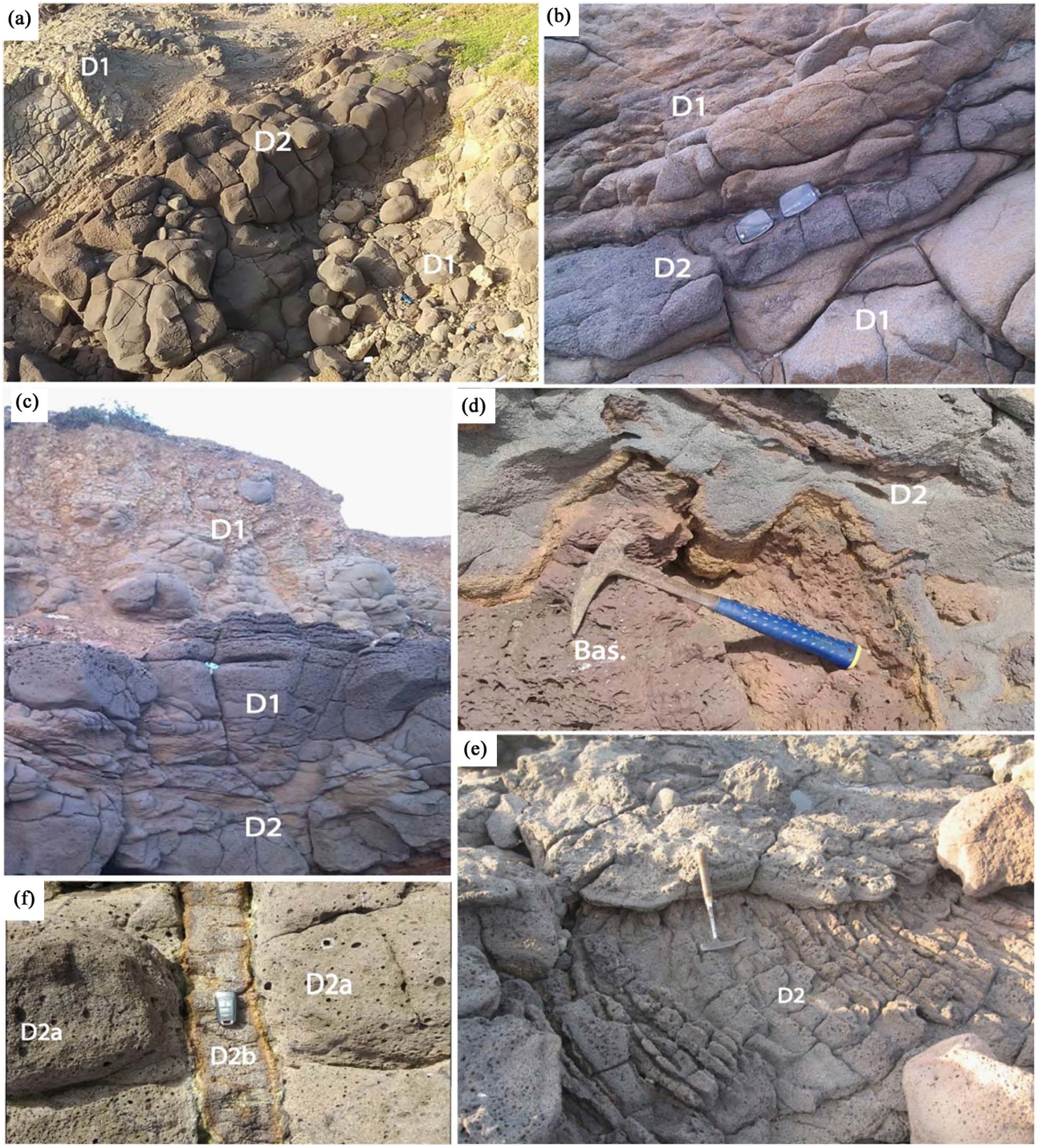

Figure 7. Fann sector lithology: (a) D2 dolerite dyke oriented N50 cutting the D1 dolerite; (b) D2 dolerite sill in D1; (c) sill of D2a in D1; (d) intrusion of basanite in the D2 dolerite and development of a contact metamorphism aureole in the latter; (e) dolerite D2 in corded lavas, observed near the university; (f) vesicular D2a dolerite intersected by another non-vesicular D2b dolerite.

and sills (Figure 7(c)).

The contact between D1 and D2 is marked by a halo of contact metamorphism. Between the "Place du Souvenir" and the tip of the residence of the Embassy of Mali, dolerites D1 and D2 are cut by a vacuolar basanite. A halo of

thermal metamorphism has developed in these dolerites (Figure 7(d)). The IFAN Cheikh Anta Diop beach offers many outcrops of D2 dolerite, which can also occur in the form of corded lava (Figure 7(e)). There are also late injections of less vesicular D2 dolerite (Figure 7(f)). Under the microscope, D1 dolerite presents an inter-granular doleritic texture marked by contiguous plagioclase laths making between them interstices occupied by pyroxene and olivine minerals (Figure 8(a)) and a sub-doleritic texture with laths of partially contiguous plagioclases. D2 dolerite shows under the microscope a coarser intergranular doleritic texture (Figure 8(b)) and a subophitic texture. The mineralogical composition of the D1 and D2 dolerites is identical. The primary paragenesis consists of plagioclases, pyroxenes and olivines. The secondary alteration paragenesisis formed of iddingsite, chlorite, epidote and opaque minerals. The mineral mode varies according to the samples with a predominance of either plagioclase or pyroxene.

Moreover, in the blades cut on the samples of dolerites having undergone thermal metamorphism in contact with the basanite, the ferromagnesian minerals

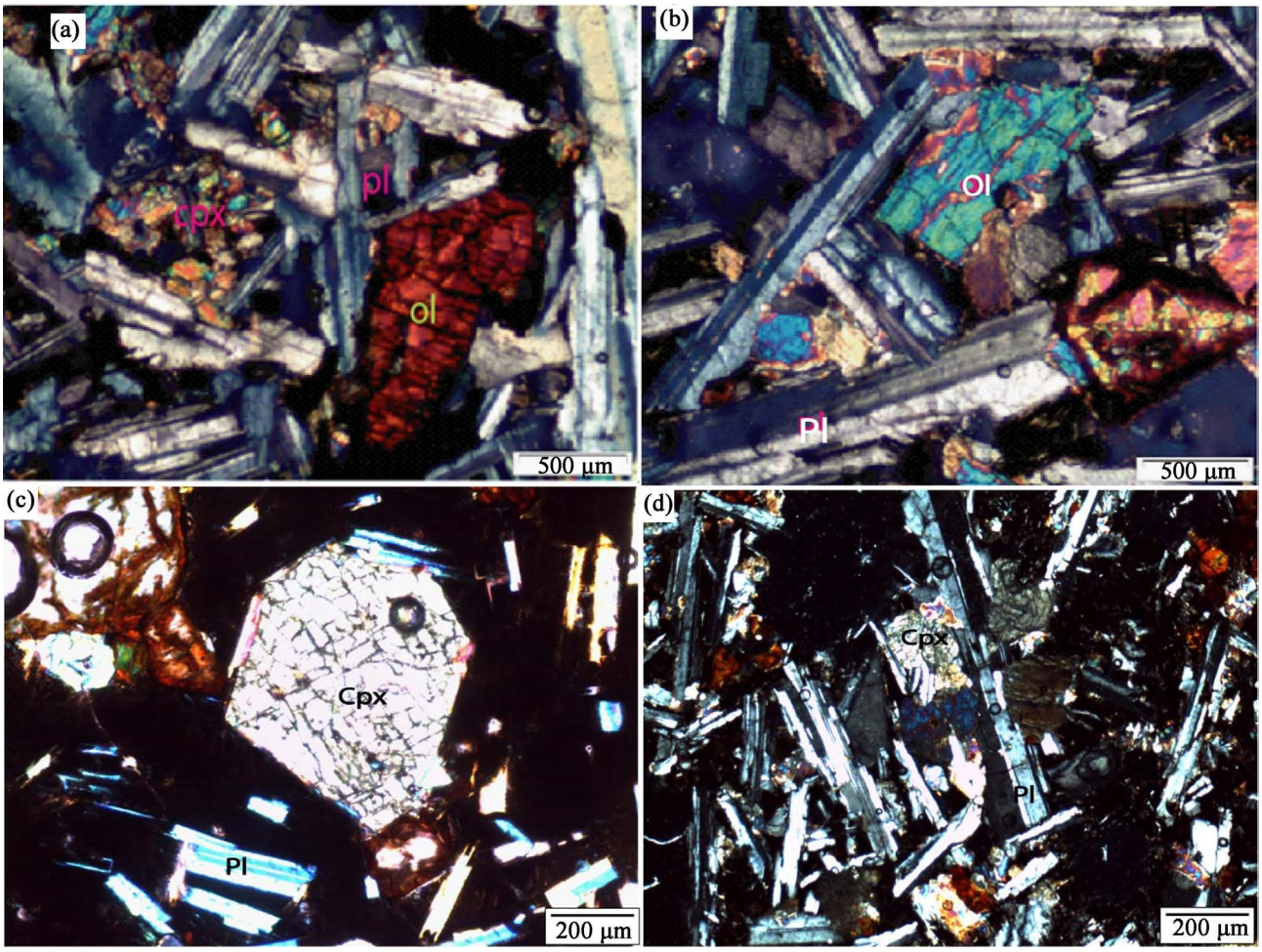

Figure 8. Petrography of the Fann sector: (a) dolerite D1 (MF177A) showing contiguous plagioclase laths, between which we see olivine and pyroxene minerals; (b) dolerite D2 in dyke (MF221A) showing contiguous plagioclase laths, between which we see olivine and pyroxene minerals; (c) dolerite D1 (MF308) showing destabilization of primary minerals to opaque minerals; (d) dolerite D2 in dyke (MF221B) showing destabilization of primary minerals to opaque minerals (Op).

are very strongly opacified (Figure 8(c), Figure 8(d)).

- **Basanites**

They outcrop between the point of the place of remembrance and that of the residence of the Embassy of Mali. The basanite of the Place du Souvenir was emplaced along an EW axis that could correspond to oceanic transform faults. It is cut into a prism (Figure 9(a)) whose diameter varies between 15 and 80 cm.

Figure 9. Lithology in the Fann sector: (a) subvertical basanite prisms observed at Place du Souvenir; (b) dykes (Dy.) of basanite which crosscut the monogenic breccia and intrude as sills (sil.) in the dolerite; (c) enclave of gabbro (Gab.) in prismatic basanite; (d) enclave of tuff in prismatic basanite; (e) intrusion of vacuolar basanite in the D2 dolerite and development of a contact metamorphism aureole in the latter; and (f) intrusion of vacuolar basanite into Dolerite D1.

The exit point is therefore currently inside the ocean. During its advance, the basanite came up against a doleritic relief and spread on both sides of it. However, part of the lava was injected into the underlying tuffs, thus giving rise to veins (**Figure 9(b)**). This basanite contains enclaves of gabbros (**Figure 9(c)**) and metamorphosed tuffs (**Figure 10(d)**). Its superficial part is often very vesicular.

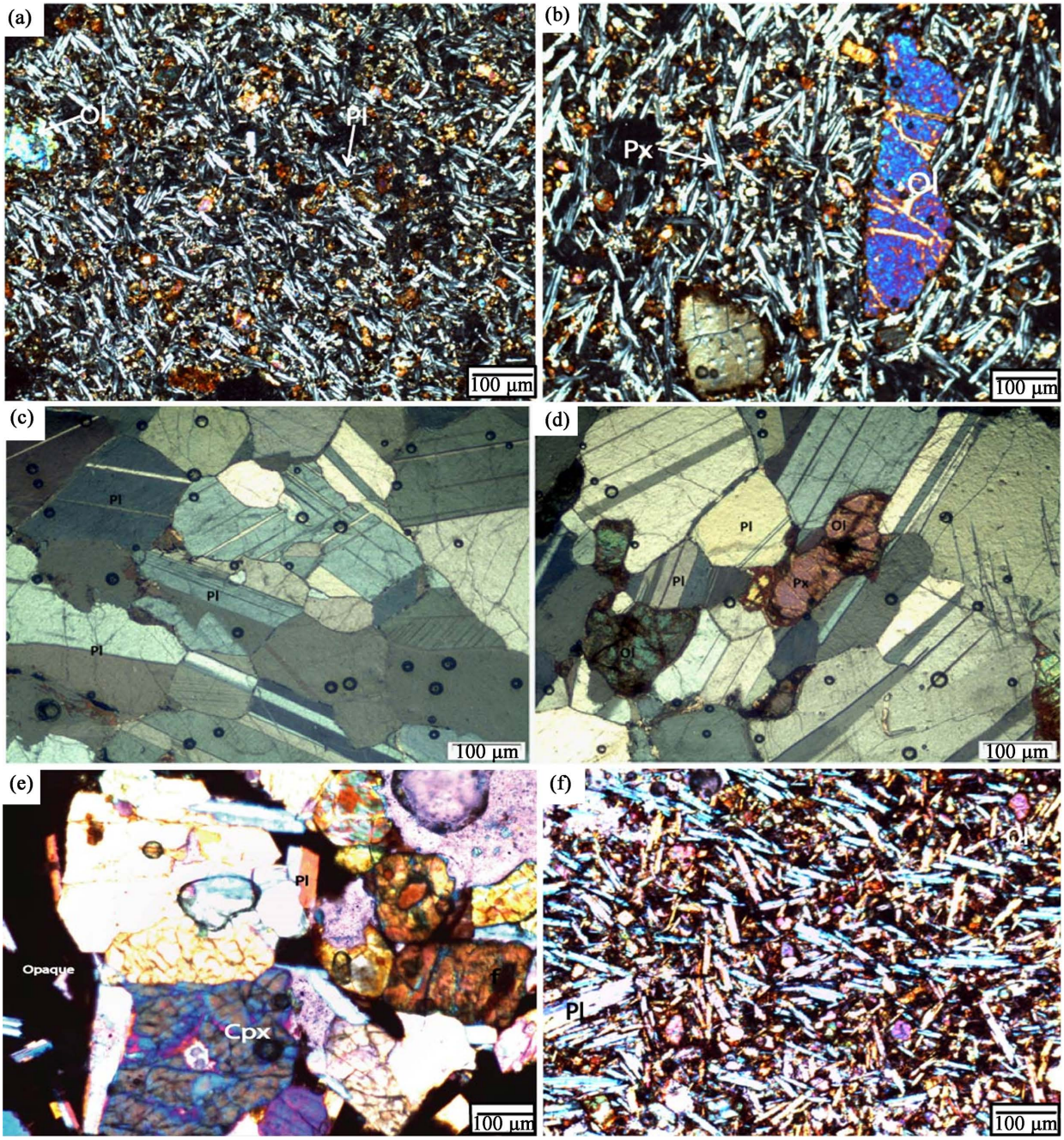

Figure 10. Lithology and petrography of the Fann sector: (a) Porphyritic microlithic texture of prism basanite (MF161) with olivine phenocrysts, pyroxene microcrystals and plagioclases (Pl); (b) porphyritic microlite texture of vacuolar basanite (MF171B) with olivine (Ol), pyroxene (px) phenocrysts and plagioclase (Pl) microlites; (c) and (d) grainy texture of the gabbro enclave (MF162) with olivine (Ol), pyroxene (Px) and plagioclase (Pl) phenocrysts; (e) subophitic doleritic texture of the polygenic breccia element (MF293B) and (f) porphyritic microlithic texture of the polygenic volcanic breccia element (MF293A).

Between the Place du Souvenir and the tip of the residence of the Embassy of Mali, the basanite is very vacuolar (**Figure 9(e)**). As in the previous case, the outflow point of the flow seems to be at sea. The lava then abutted against the doleritic reliefs (D1 and D2) metamorphosing them (**Figure 9(f)**). At the tip of the residence of the Embassy of Mali, we note that the placement of the basanite was facilitated by a fault oriented N50 and the lava after having abutted against the hitherto doleritic tip propagated laterally from either side of it. The vacuoles present in this basanite are generally sub-circular but can become elliptical at the level of contact with the dolerite. They are often empty but sometimes filled with carbonate. This carbonate is in the form of a nodule or fine whitish needles. The basanite flow contains enclaves of dolerites and tuffs. Microscopic observation of the basanite in prisms shows a porphyritic microlithic texture (**Figure 10(a)**). Olivine phenocrysts are observed embedded in a mesostasis consisting of microlites of plagioclases, pyroxenes, olivines and secondary minerals (epidote, opaque minerals). The vacuolar basanite shows under the microscope a porphyritic microlithic texture with a doleritic tendency (**Figure 10(b)**). The primary paragenesis consists mainly of plagioclase, pyroxene and olivine while the secondary alteration paragenesis is represented by carbonates and opaque minerals. The pyroxene phenocrysts show two very sharp 90˚ cleavage directions and corroded surfaces. Plagioclases, which are very abundant, form laths of microlites with sometimes polysynthetic twins. The very abundant carbonates, recognizable by their diamond-shaped cleavage, are destabilization products of pyroxenes and/or plagioclases. They are often associated with opaque needle-like minerals. The gabbro enclaves present in the prismatic basanite show a grainy texture and a mineralogical composition consisting of clinopyroxenes, plagioclases and olivines (**Figure 10(c)**).

- **The Late breccia**

A second generation of volcanic breccia outcrops south of "Place du Souvenir". This breach could represent the ultimate manifestation of volcanic activity in the Fann sector. It is polygenic and is essentially made up of heterometric fragments of dolerites and basanites united by clay cement (**Figure 10(d)**).The microscopic study of the dolerite elements shows an intergranular texture (**Figure 10(e)**). The basanite fragments show a porphyritic microlithic texture (**Figure 10(f)**).

The fragments present the same mineralogical composition consisting of olivine, pyroxenes, plagioclases and opaque minerals.

4.2. Tectonic Structures

The placement of volcanic rocks in the Mermoz and Fann sectors is intimately linked to tectonic structures.

4.2.1. The Mermoz Sector

The main emission zone is a collapsed crater located at the intersection of three

large fractures: NE-SW (N40), NW-SE (N140) and N-S (**Figure 11(a)**, **Figure 11(b)**). The NE-SW fractures allowed the placement of basanites, which are moreover oriented in this direction (**Figure 11(a)**). In the crater, the NE-SW alignment of breccias within the basanites themselves undoubtedly indicates that the fractures oriented in this direction were the site of an explosion. In addition, in the eastern part of the volcano, the explosions at the origin of the clear volcanic breccia also occurred along a NE-SW axis. The NW-SE fractures, for their part, are essentially associated with the setting up of the late breccias (**Figure 11(c)**), which can be followed over several tens of meters in the N140 direction. All these fractures are vertical to subvertical. Their directions of movement are not always easy to determine. However, dextral and sinistral movements were noted in NE-SW shear corridors (**Figure 11(c)**), while essentially sinistral movement was recorded on NW-SE and NS fractures. Thin sections of intensely fractured rocks show a very clear orientation of feldspars. After the setting of late breccias, the Mermoz volcano underwent a major collapse illustrated by streaks of landslides plunging 50˚ at N140 (**Figure 11(c)**). This collapse is at the origin of a depression at the current location of the crater. The volcanic rocks of the Mermoz sector recorded a final phase of brittle tectonics at the origin of E-W structures which intersect the N40, N140 and NS fractures. A statistical study of the main fracture directions indicates a predominance of those oriented NE-SW and NW-SE (**Figure 12(a)**) and a predominance NE-SW for the veins (**Figure 12(b)**).

4.2.2. The Fann Sector

No emerged crater related to volcanic products from the Fann sector was observed. The main exit points for basanites are currently in the ocean. These were only able to reach the coast via the E-W faults (Place du Souvenir, **Figure 13(a)**) or the NE-SW faults (Residence of the Embassy of Mali, **Figure 13(b)**). The mode of emplacement of the D1 dolerite is not always clear, but the way in which it extends offshore seems to indicate that these are veins emplaced in NE-SW and E-W fractures. The second generation dolerites are also emplaced through the fractures oriented NE-SW, E-W and N-S, which mainly affect the D1 dolerite (**Figure 13(d)**). These fractures reappeared later and mainly affected the walls of the D2 dolerite veins (**Figure 13(c)**). A statistical study of the main fracture directions indicates a predominance of those oriented NE-SW and NW-SE (**Figure 14(a)**) and a predominance NE-SW (**Figure 14(b)**) for the veins.

4.3. Geochemistry

Geochemical analyzes in major and trace elements were carried out on 9 samples, 6 of which belong to the Fann sector and 3 to the Mermoz sector (**Table 1**). In this study, rare earth element (REE) concentrations are normalized to the NWA974 chondrites of [24] and extended trace element concentrations are normalized to the early mantle from [25].

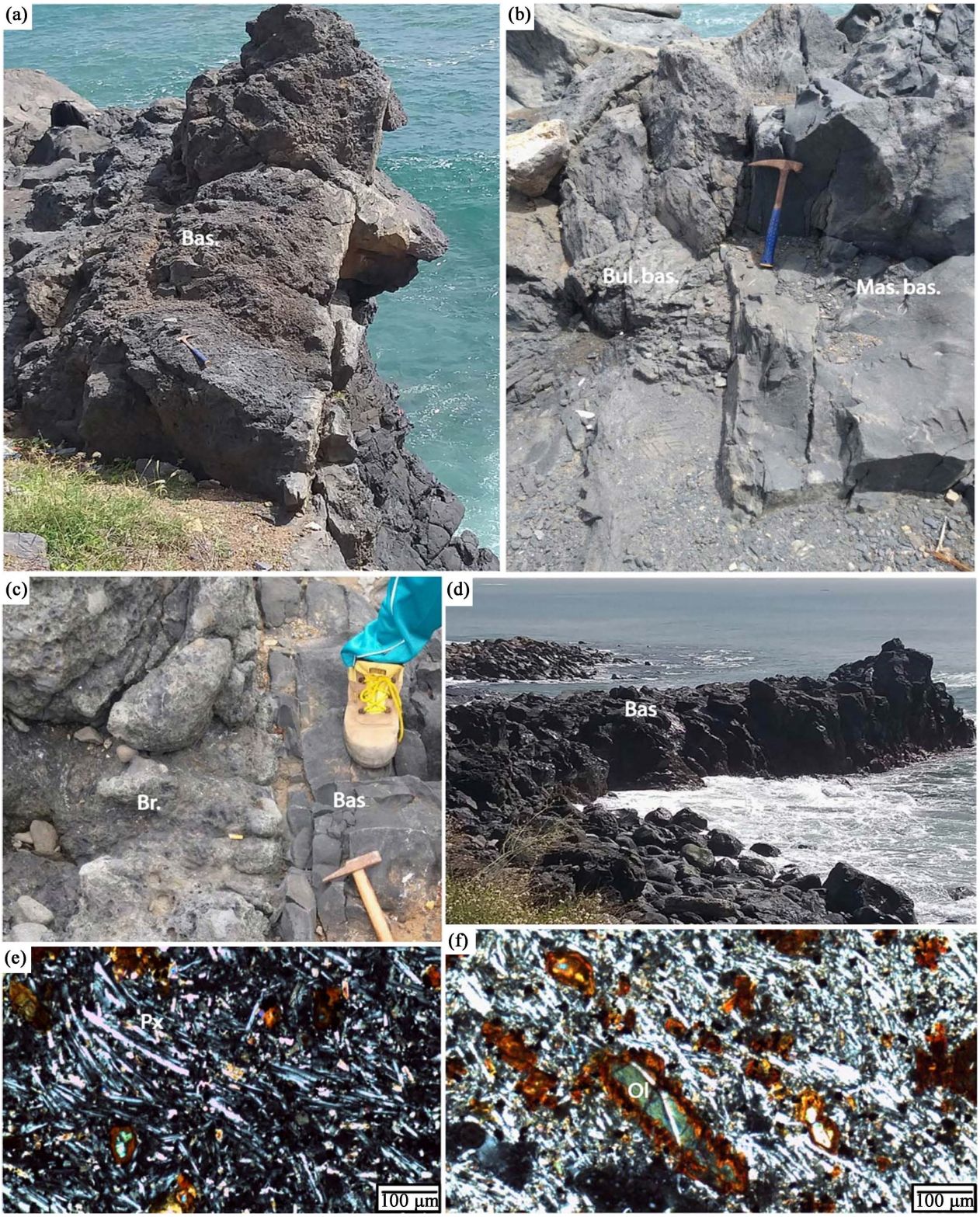

Figure 11. Deformations in the Mermoz sector: (a) N-S trending fracture at the eastern end of the crater; (b) N10 trending fracture zone at the eastern edge of the crater. (c) Fracture N140 that facilitated the placement of the late breach; (d) the elongated massive basanite flow along the N40 direction; (e) Sinistral N40 strike-slip observed in a thin section of massive basalt with plagioclase oriented in the same direction and (f) sinistral N40 shear observed in a thin section with olivines and plagioclases oriented in the same direction.

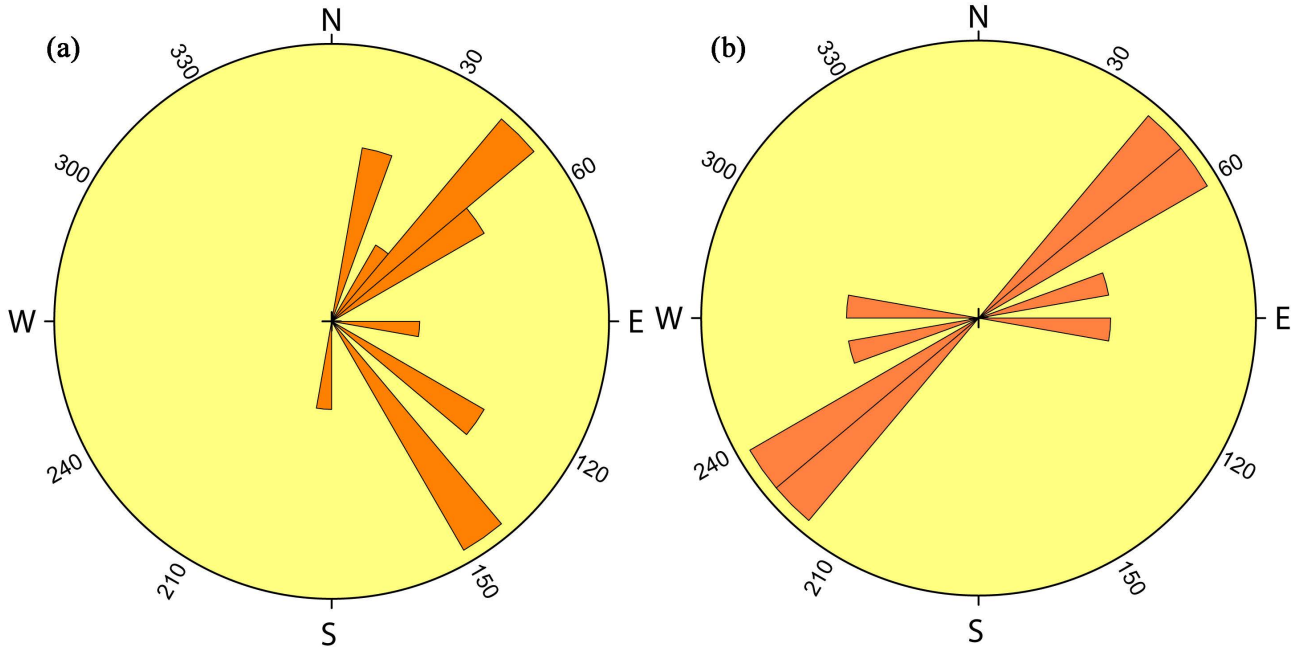

Figure 12. (a) Rose diagram showing the preferential orientation of the fracture planes in the Mermoz sector and (b) rosette showing the preferential orientation of the directions of the veins in the Mermoz sector.

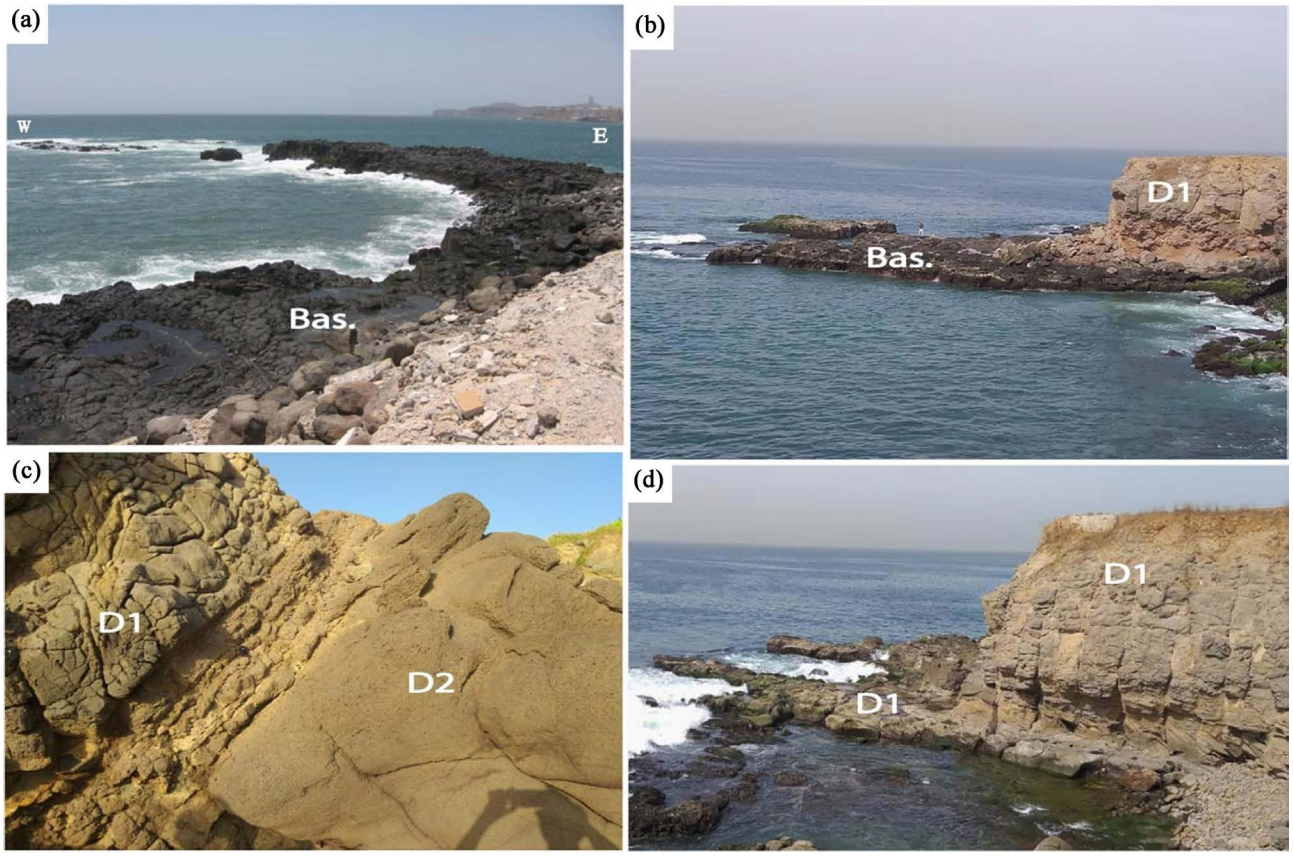

Figure 13. Deformations in the Fann sector: (a) outcrop of prismatic basanite (Bas.) extending into the ocean in an E-W direction; (b) extension into the ocean of the point of the Embassy of Mali oriented in a direction N40; (c) faulted contact between dolerite D1 and dolerite D2 and (d) extension into the ocean of a dolerite vein oriented N40.

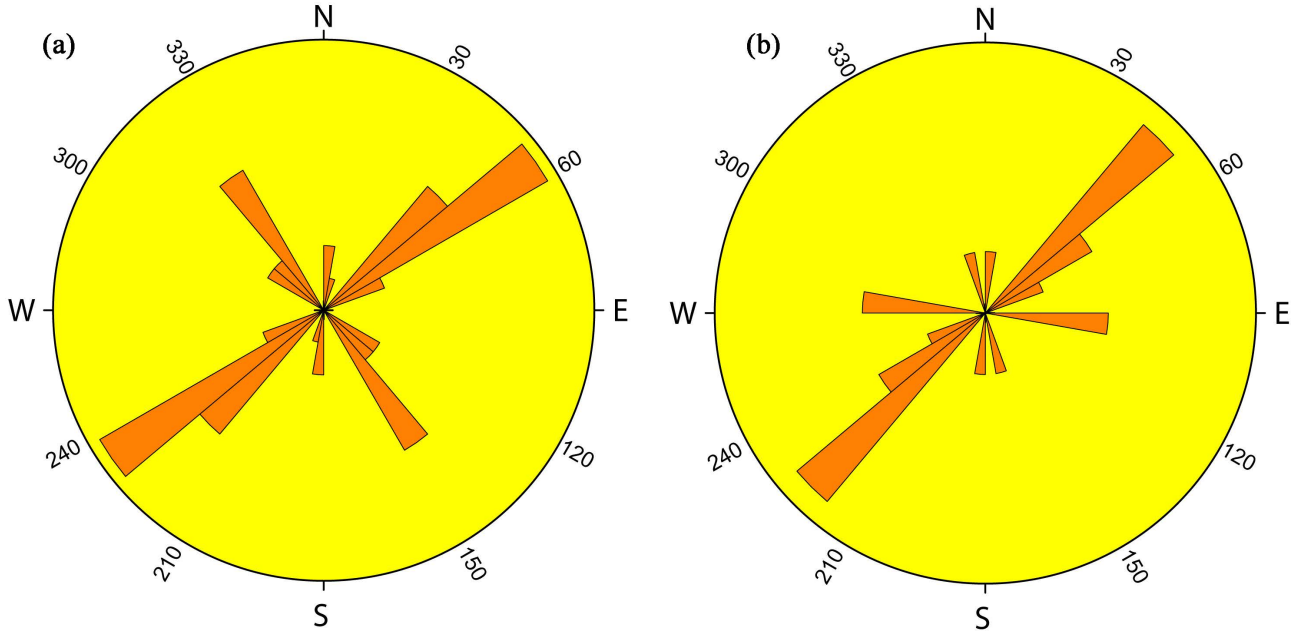

Figure 14. (a) Rose diagram showing the preferential orientation of the planes of the diaclases in the Fann sector and (b) rose diagram showing the preferential orientation of the vein directions in the Fann sector.

4.3.1. The Major Elements

In the Fann sector, the SiO_2, Al_2O_3, TiO_2, MgO, Fe_2O_3(T), CaO, Na_2O, K_2O, P_2O_5 and Mg# values vary respectively from 52.5% - 53%, 14.6% - 14.8%, 1.5% - 1.6%, 5.2% - 6.3%, 10.7% - 11%, 8.3% - 9%, 3.9% - 4%, 0.5% - 0.7%, 0.31% - 0.41% and 48.5% - 53.9% in dolerites and 48.3% - 49%, 14.2% - 14.8%, 1.7% - 1.9%, 7.1% - 8.2%, 9.8% - 11%, 8.7% - 10.1%, 3.6% - 4.2%, 1.2% - 1.5%, 0.44% - 0.53% and 57.2% - 59.5% in basanites. It should be noted, however, that D1 dolerite (MF177B) and D2 dolerite (MF157B) are slightly richer in SiO_2 (52.9% - 53% compared to 52.5%) and in K_2O (0.6-0.7% against 0.5%) but slightly less rich in TiO_2 (1.5% against 1.6%), Na_2O (3.9% against 4%) and P_2O_5 (0.3% against 0.4%) than D2 dolerite (MF221B) (**Figure 15(a)**, **Figure 15(b)**, **Figure 15(e)**, **Figure 15(f)**).

In the Mermoz sector, the SiO_2, Al_2O_3, TiO_2, MgO, FeO(T), CaO, Na_2O, K_2O, P_2O_5 and Mg# contents vary respectively from 50.6% - 52.4%, 14% - 15.8%, 1.8% - 2.9%, 3.3% - 5.6%, 12% - 12.9%, 7.3% - 8.1%, 4.3% - 4.8%, 1% - 1.5%, 0.3% - 0.5% and 33.8% - 47.9% in the dolerites and equal respectively to 49.4%, 14.7%, 1.9%, 7.7%, 10.8%, 8.5%, 4.7%, 1.5%, 0.58% and 58.7 in basanite.

Fann dolerites show slightly higher values of SiO_2 (52.5% - 53% versus 50.6% - 52.4%), CaO (8.3% - 9%) and Mg# (48.5 - 53.9 against 33.8 to 47.9) but lower values in TiO_2 (1.5% - 1.6% against 1.8% - 2.9%), Fe_2O_3(T) (10.7% - 11% against 12% - 12.9%), Na_2O (3.9% - 4% versus 4.3% - 4.8%) and K_2O (0.5% - 0.7% versus 1% - 1.5%) than the Mermoz dolerites (**Figure 15(a)**, **Figure 15(b)**, **Figure 15(d)**, **Figure 15(e)**, **Figure 15(f)**). In addition, dolerites from both sectors show poor correlations with Mg#, negative for TiO_2, Na_2O and K_2O (**Figure 15(b)**, **Figure 15(e)**, **Figure 15(f)**) and positive for CaO (**Figure 15(d)**). These

Table 1. Majors and traces elements of the totals dolerites and basanites rocks of the Fann and Mermoz sectors.

Sector	Fann			Mermoz					
Lithology	Dolerite 1	Dolerite 2		Prismatic basanite			Dolerite		Basanite
Sample	MF177B	MF157B	MF221	MF161	MF171A	MF175	MF199	MF202	MF200
SiO_2	52.95	52.97	52.48	48.88	49.04	48.3	52.45	50.62	49.43
TiO_2	1.46	1.55	1.6	1.9	1.81	1.7	2.9	1.78	1.88
Al_2O_3	14.56	14.78	14.8	14.78	14.61	14.22	13.96	15.77	14.68
Fe_2O_3(T)	10.73	11.04	10.86	10.88	11.03	9.77	12.9	11.99	10.81
MnO	0.14	0.11	0.13	0.14	0.13	0.14	0.14	0.16	0.14
MgO	6.33	5.24	5.63	7.33	8.18	7.09	3.33	5.57	7.75
CaO	9.03	8.27	8.92	8.68	8.73	10.08	7.33	8.14	8.51
Na_2O	3.87	3.93	4	4.19	3.58	3.58	4.8	4.27	4.68
K_2O	0.64	0.69	0.5	1.49	1.26	1.18	1.54	0.96	1.53
P_2O_5	0.31	0.34	0.41	0.53	0.48	0.44	0.55	0.31	0.58
LOI	0.63	1.59	1.21	1.76	1.5	3.73	0.55	1.05	0.44
Total	100.7	100.5	100.5	100.6	100.4	100.2	100.4	100.6	100.4
Mg#	53.89	48.46	50.67	57.17	59.50	58.98	33.84	47.92	58.68
Ni	170	150	120	230	300	250	50	200	250
Cr	290	280	260	300	360	300	100	280	340
Co	42	38	36	41	44	40	31	52	43
V	144	143	152	150	156	150	222	163	147
Cs	0.1	0.2	0.2	0.3	0.2	0.2	0.4	0.1	0.5
Rb	14	13	12	38	31	24	37	18	43
Ba	340	307	323	578	496	443	516	403	542
Th	3.06	3.48	3.15	4.13	3.92	3.18	4.27	2.52	4.27
U	0.49	0.83	0.86	0.91	0.82	0.68	0.4	0.33	1.04
Nb	32.5	34	31.9	53.1	48.5	41.5	56	32.3	53.9
La	26.4	33.9	29.2	34.1	32.8	27.6	31.8	21.4	35.2
Ce	44.8	52.8	45.4	58.7	56.1	48.4	56.5	35.1	59.9
Pr	5.15	6.29	5.43	6.94	6,56	5,73	7,09	4,74	7,03
Sr	508	459	485	800	731	703	398	502	738
Nd	20.2	25.9	21.5	28.3	27.7	24	30.9	20.7	29.3
Zr	82	88	89	145	130	125	157	97	141
Sm	4.48	5.62	4.85	6.41	6.14	5.51	7.57	4.93	6.33
Eu	1.59	1.91	1.64	2.12	2.03	1.87	2.51	1.79	2.19
Gd	4.57	6.01	4.96	5.91	5.61	4.96	8.04	5.25	5.91
Dy	3.72	4.78	4.05	4.38	4.16	3.87	6.43	4.13	4.45
Ho	0.65	0.86	0.71	0.74	0.69	0.66	1.15	0.73	0.75
Er	1.59	2.16	1.76	1.8	1.64	1.66	2.9	1.78	1.87
Y	17.5	25.2	20.9	19.9	19.2	18.1	33.2	20.5	20.3
Yb	1.21	1.54	1.35	1.31	1.2	1.18	2.14	1.31	1.36
Lu	0.18	0.22	0.21	0.19	0.18	0.17	0.3	0.19	0.19
Sn	2	3	2	3	2	2	3	1	3
Tb	0.69	0.9	0.76	0.84	0.8	0.76	1.18	0.78	0.84
W	< 0.5	0.8	< 0.5	0.8	0.8	0.5	0.7	14.2	1.4
Ta	1.69	1.75	1.56	3.35	2.96	2.45	3.65	2.11	3.45
Mo	4	4	4	5	4	4	5	3	7
Hf	2.3	2.4	2.3	3.6	3.2	2.9	4.6	2.8	3.5
ΣREE	652.45	819.68	699.52	855.1	818.22	718.73	941.41	618.24	872.67
La_N/Yb_N	20.57	20.76	20.4	24.55	25.78	22.06	14.01	15.40	24.41
La_N/Sm_N	4.21	4.31	4.31	3.8	3.82	3.58	3	3.10	3.98
Gd_N/Yb_N	3.61	3.73	3.51	4.31	4.46	4.01	3.59	3.83	4.15
La_N/Nd_N	2.84	2.85	2.96	2.62	2.58	2.5	2.24	2.25	2.62
Sm_N/Gd_N	1.35	1.29	1.35	1.5	1.51	1.53	1.3	1.3	1.48
Dy_N/Lu_N	2.4	2.55	2.29	2.71	2.75	2.77	2.52	2.64	2.8
Eu/Eu*	0.94	0.88	0.89	0.91	0.92	0.95	0.86	0.94	0.95

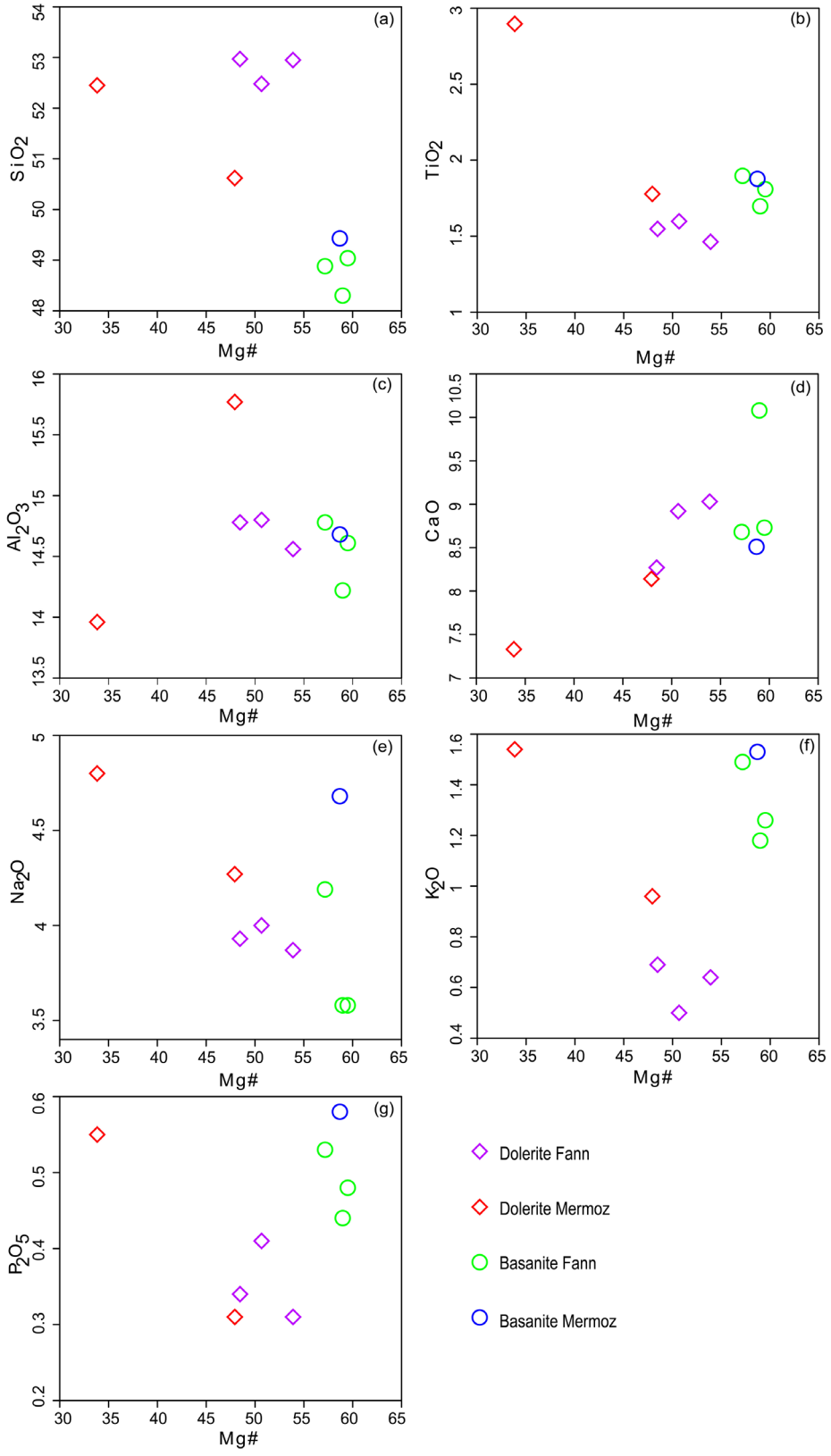

Figure 15. Diagrams of SiO_2, TiO_2, Al_2O_3, CaO, Na_2O, K_2O and P_2O_5 as a function of Mg# showing the variations in composition of the major elements of the dolerites and basanites of the Fann and Mermoz sectors.

geochemical characteristics suggest that the dolerites of the two sectors could come from the same magmatic source. Furthermore, Fann basanites are also slightly richer in CaO (8.7% - 10.1% vs. 8.5%) but slightly poorer in SiO_2 (48.3% - 49% vs. 49.4%), Na_2O (3.6% - 4.2% versus 4.7%), K_2O (1.2% - 1.5% versus 1.53%) and P_2O_5 (0.4% - 0.5% versus 0.6%) than Mermoz basanite (**Figure 15(a)**, **Figures 15(d)-(g)**). It should also be noted that the basanites of the two sectors show very similar chemical compositions, probably indicating a single magmatic source. Finally, the dolerites of the two sectors compared to the basanites of the two sectors are richer in SiO_2 (50.6% - 53% against 48.3% - 49.4%) but poorer in MgO (3.3% - 6.3% against 7.1% - 8.2%) and Mg# (33.8% - 53.9% versus 57.2% - 59.5%) (**Figure 15(a)**). These chemical characteristics as well as the absence of correlations between dolerites and basanites and the presence of enclaves of dolerites in basanites suggest different magmatic sources.

The quaternary basanites in this study show the same geochemical characteristics as the quaternary basanite analyzed by [26] in the Mermoz sector (**Figure 16**, **Figure 18(a)**, **Figure 18(b)**).

Furthermore, the Quaternary lavas from this study were compared to the Quaternary lavas from well-known sites such as Fogo Island in Cape Verde [27] and Réunion Island in France [28].

This comparison shows that the lavas of this study have geochemical characteristics (major and traces) very different from those of these oceanic islands (**Figure 16**, **Figure 18(a)**, **Figure 18(b)**). Indeed, the major elements are different, the lavas of this study being richer in SiO_2 (48.3% - 49.4% against 40.6% - 42.5%) and Mg# (57.2 - 59.5 against 46.8 - 56.3) but poorer in TiO_2 (1.7% - 1.9% versus 3.5% - 4.4%), CaO (8.5% - 10.1% versus 11.1% - 12.8%), Fe_2O_3(T) (9.8% - 11% versus 13.1% - 14.2%), K_2O (1.2% - 1.5% versus 1.9% - 2.8%), MnO (0.13% - 0.14% vs. 0.18% - 0.21%) and P_2O_5 (0.4% - 0.6% vs. 0.6% - 0.9%) than Fogo lavas. In addition, the lavas in this study are also richer in SiO_2 (48.3% - 49.4% versus 47.1% - 47.6%), Na_2O (3.6% - 4.7% versus 2.2% - 3.4%), K_2O (1.2% - 1.5% vs. 0.5% - 0.9%), MnO (0.13% - 0.14% vs. 0.10% - 0.11%) and P_2O_5 (0.4% - 0.6% against 0.1% - 0.3%) but poorer in TiO_2 (1.7% - 1.9% against 2.6% - 3.5%) and Fe_2O_3(T) (9.8% - 11% against 12.4% - 13.2%) than lava from Réunion.

4.3.2. Trace Elements

In the Fann sector, compatible elements such as Ni, Cr, Co and V vary respectively from 120 - 170 ppm, from 260 - 270 ppm, from 36 - 42 ppm and from 143 - 152 ppm in the dolerites and from 230 - 300 ppm, from 300 - 360 ppm, from 40 - 44 ppm and from 150 - 156 ppm in basanites. Incompatible elements such as Nb, Zr and Y vary respectively between 31.9 - 34 ppm, 82 - 89 ppm and 17.5 - 25.2 ppm in the dolerites and between 41.5 - 53.1 ppm, 125 - 145 ppm and 18.1 - 19.9 ppm in basanites.

In the Mermoz sector, the concentrations of compatible elements such as Ni, Cr, Co and V vary greatly respectively from 50 - 200 ppm, from 100 - 280 ppm, from 31 - 52 ppm and from 163 - 222 ppm in the dolerites and are respectively

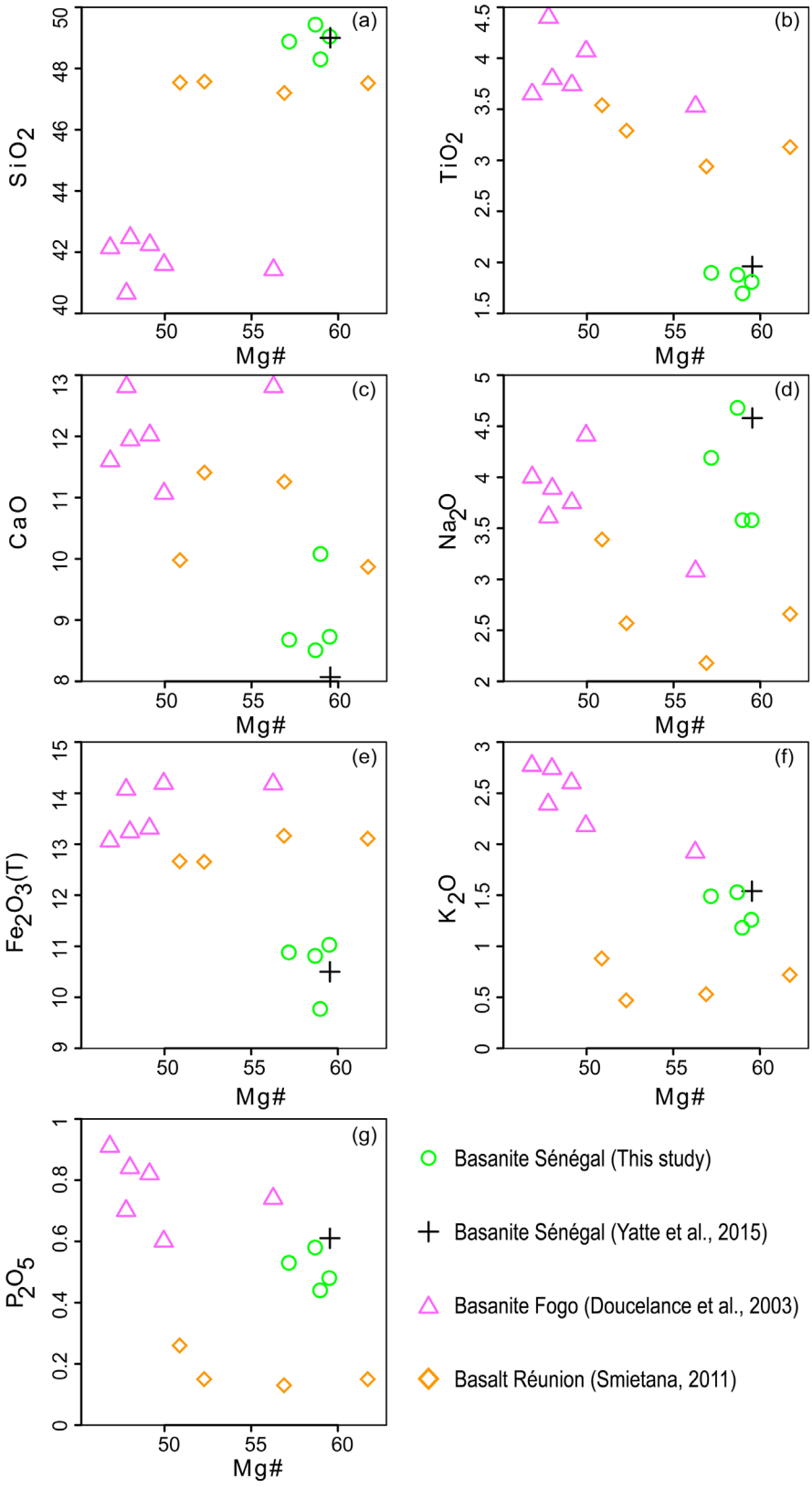

Figure 16. Diagrams of SiO_2, TiO_2, CaO, Na_2O, FeO_3 (T), K_2O and P_2O_5 as a function of Mg# showing the comparison of Quaternary lava from Senegal with that of equivalent lava from the Fogo islands (Cape Verde) and Réunion (France).

equal to 250 ppm, 340 ppm, 43 ppm and 147 ppm in the basanites. Incompatible elements like Nb, Zr and Y also vary a lot in the dolerites respectively between 32.3 - 56 ppm, 97 - 157 ppm and 20.5 - 33.2 and equal respectively to 53.9 ppm, 141 ppm and 20.3 ppm in basanites.

In conclusion, the Ni and Cr contents are higher in the basanites than in the dolerites and this is undoubtedly linked to the abundance of olivine crystals in the basanites unlike the dolerites, which contain very little.

4.3.3. Rare Earths Elements

Fann dolerites with ΣREE = 652 - 820 ppm are very enriched in LREE by 106 to 215 times the chondrites and very depleted in HREE by 8 to 9 times the chondrites. This results in very steep REE spectra (La_N/Yb_N = 20.4 - 20.8) marked by a progressive depletion of LREE (La_N/Nd_N = 2.8 - 3) towards HREE (Dy_N/Lu_N = 2.3 - 2.5) passing through the MREEs (Sm_N/Gd_N = 1.3 - 1.4) with very slight negative anomalies in europium (Eu/Eu^* = 0.88 - 0.94) (**Figure 17(a)**). However,

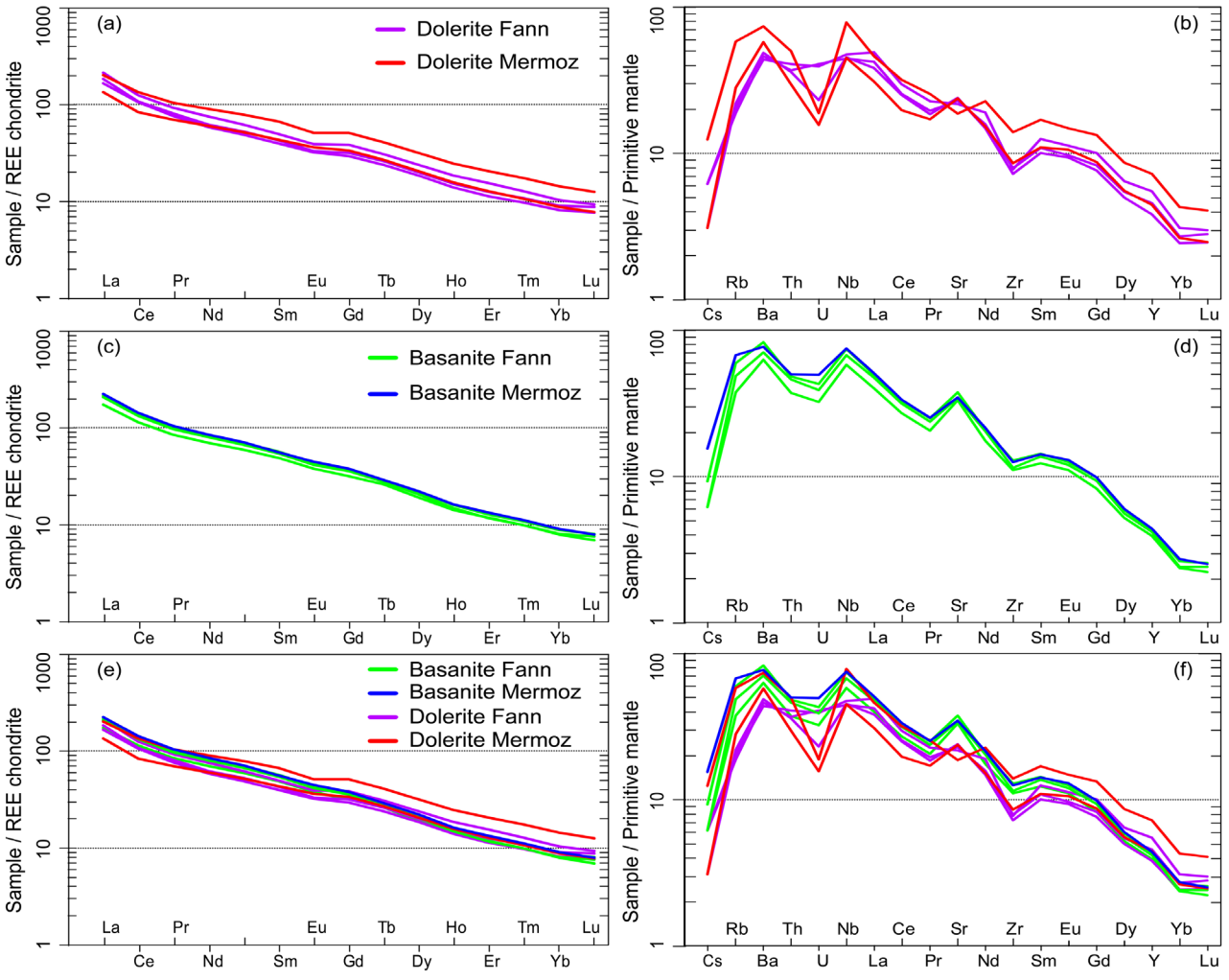

Figure 17. ((a), (c) and (e)) diagrams showing the spectra of rare earths normalized to NWA974 chondrites [26] and ((b), (d) and (f)) multi-element diagrams of incompatible elements normalized to the primitive mantle [27] dolerites and basanites from the Fann and Mermoz sectors.

it should be noted that the D2 dolerite has an intermediate chemical composition between the two samples of D1 dolerites. On the enlarged diagram normalized to the primitive mantle (**Figure 17(b)**), all the dolerites present enrichment in LILEs (Large Ion Lithophilic Elements) (Cs, Rb, Ba) and negative anomalies in Pr, Zr and Yb and positive in Sr.

Mermoz dolerites with ΣREE = 618 - 941 ppm show quite similar REE spectra with the same fractionation as Fann dolerites. They are enriched by 135 to 201 times the chondrites in LREE (La_N/Nd_N = 2.2 - 2.3) and depleted by 8 to 13 times the chondrites in HREE (Dy_N/Lu_N= 2.5 - 2.6) with very steep spectra (La_N/Yb_N = 14 - 15.4) and very slight negative anomalies (Eu/Eu* = 0.86 - 0.94) (**Figure 17(a)**). On the enlarged diagram normalized to the primitive mantle (**Figure 17(b)**), we observe enrichment in LILEs and very marked negative anomalies in U and Zr and positive anomalies in Nb.

Fann basanites with ΣREE = 719 - 855 ppm are characterized by highly fractionated REE spectra (La_N/Yb_N = 22.1 - 25.8) marked by a very strong LREE enrichment (La_N/Nd_N = 2.5 - 2.6) by 175 to 216 times compared to chondrites and a net HREE depletion (Dy_N/Lu_N = 2.7 - 2.8) by 7 to 8 times compared to chondrites (**Figure 17(c)**). Europium shows very weak negative anomalies (Eu/Eu* = 0.91 - 0.95). However, the basanite in prisms is very slightly more enriched in REE than the basanites in vacuolars. On the enlarged diagram normalized to the primitive mantle (**Figure 17(d)**), the Fann basanites present an enrichment in LILEs and negative anomalies in U, Pr, Zr and Yb and positive in Nb and Sr. Mermoz basanite (ΣREE = 873 ppm) on the other hand, has a spectrum identical to the spectrum of Fann basanite. It is enriched in LREE by 223 times the chondrites with a very marked fractionation of the spectrum (La_N/Yb_N = 24.4) and a very slight negative europium anomaly (Eu/Eu* = 0.95) (**Figure 17(c)**). On the enlarged diagram normalized to the primitive mantle (**Figure 17(d)**), the Mermoz basanite also shows the same positive and negative anomalies as the Fann basanites. It should be noted that the very pronounced positive anomalies in Sr observed in the basanites of the two sectors are compatible with the abundance of plagioclases, while the negative anomalies in Zr encountered in all the samples would be linked to the fractionation of clinopyroxenes. Moreover, the REE spectra indicate, like the major elements, source heterogeneity between the dolerites and the basanites.

The REES of the Fann and Mermoz lavas were compared with those of the lavas of the Fogo and Réunion islands. The LREEs of the lavas of this study are intermediate between those of Fogo more enriched (285 to 373 times against 175 to 223 times the chondrites) and those of Réunion less enriched (79 to 170 times against 175 to 223 times the chondrites) (**Figure 18(a)**). On the other hand, with regard to the HREEs, the lavas of this study are less enriched (7 to 8 times against 10 to 13 times the chondrites for Fogo and 11 to 13 times the chondrites for Réunion) with a more marked fractionation (Dy_N/Lu_N = 2.7 - 2.8 against 2.4 - 2.7 for Fogo and 1.9 - 2.6 for Réunion) (**Figure 18(a)**). In addition, the LILEs of

the lavas in this study are intermediate between those of the Fogo and Réunion lavas while the HFSEs are less enriched (**Figure 18(b)**).

4.3.4. Magmatic Affinity

The dolerites and basanites of the Fann and Mermoz sectors are located in the alkaline basalt domain in the diagrams of [29] (**Figure 19(a)**) and [30] (**Figure 19(b)**).

4.3.5. Nature and Heterogeneity of the Magmatic Source

The position in the La/Yb (ppm) versus La (ppm) diagram of [31] (**Figure 20(a)**) of dolerites and basanites from the Fann and Mermoz sectors indicates that these rocks come from a very enriched magmatic source. This source which

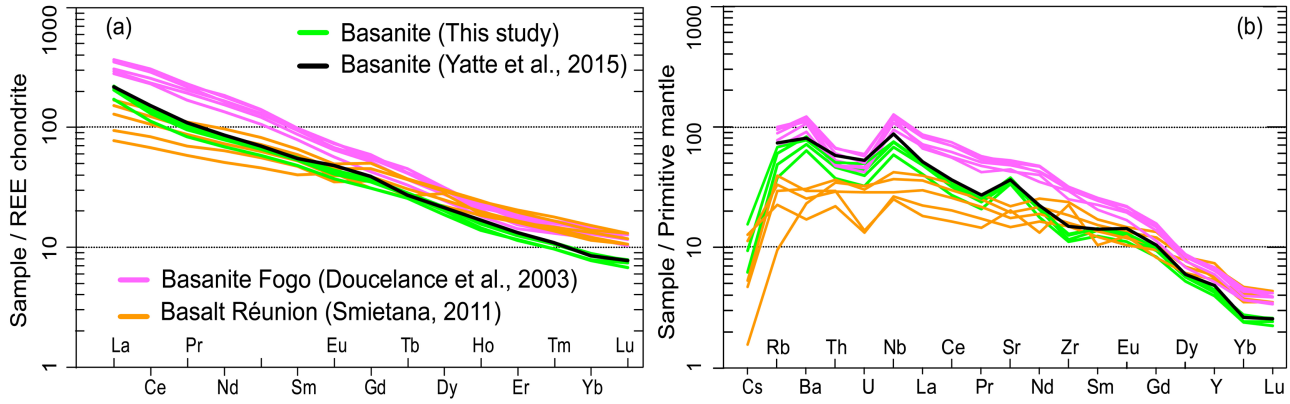

Figure 18. (a) Spectra of rare earths normalized to NWA974 chondrites [26] and (b) multi-element diagrams of incompatible elements normalized to the primitive mantle [27] of the quaternary lavas of this study compared to those of equivalent lavas in the islands of Fogo in Cape Verde and Réunion in France.

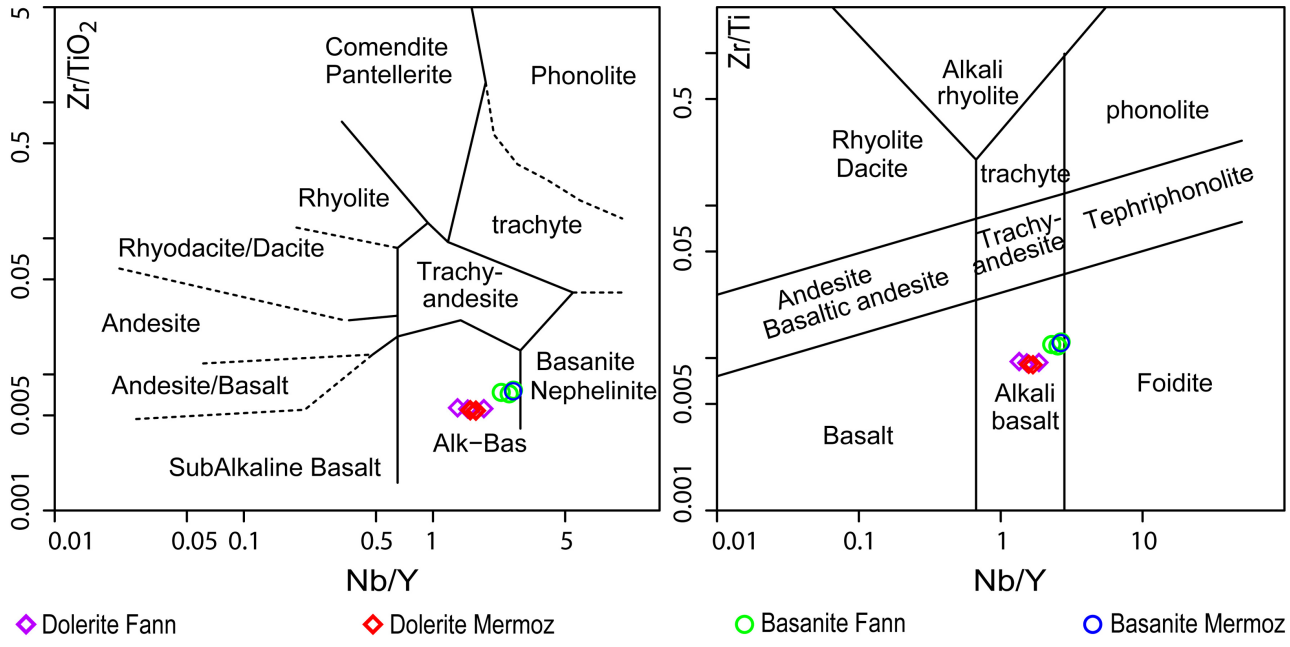

Figure 19. Diagrams from [29] (a) and [30] (b) showing the alkaline nature of dolerites and basanites in the Fann and Mermoz sectors.

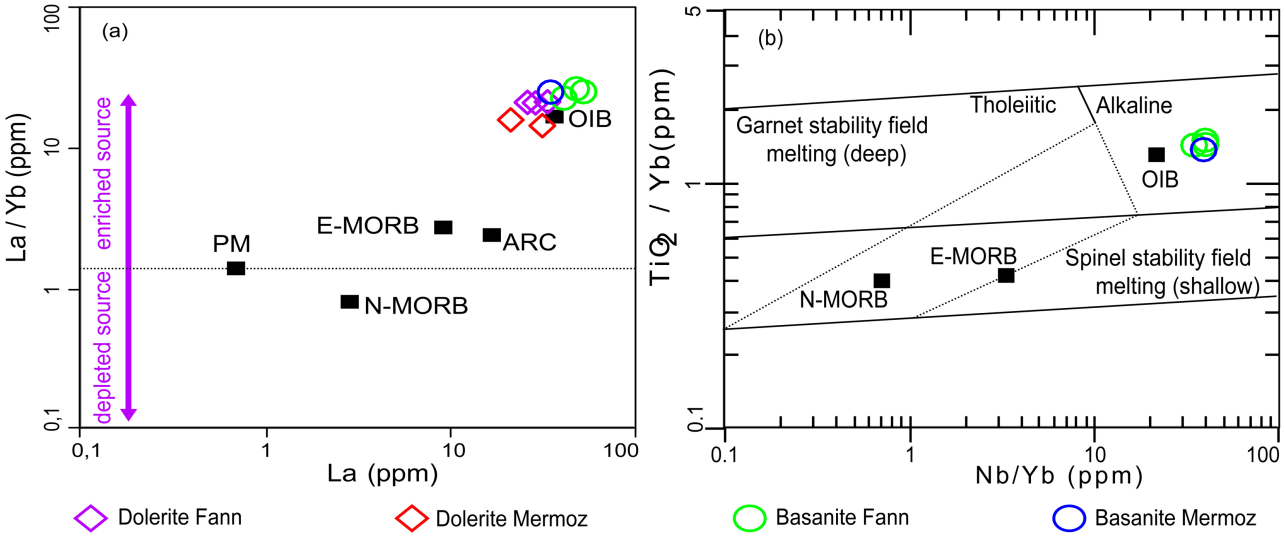

Figure 20. Diagrams: (a) La/Yb (ppm) as a function of La (ppm) from [31] and (b) TiO_2/Yb (ppm) as a function of Nb/Yb (ppm) from [32] showing the nature, heterogeneity and depth of the magmatic source of the magmatic rocks of the Fann and Mermoz sectors.

could be the same as that of the basalts of the oceanic islands (OIB) is above the values of the primitive mantle (MP), the normal residual upper mantle (N-MORB) or enriched (E-MORB) and the arc. It should be noted, however, that this diagram also confirms the heterogeneity of the source, which gave rise to the dolerites and the basanites, the latter coming from an even more enriched source. In addition, the TiO_2/Yb (ppm) versus Nb/Yb (ppm) diagram of [32] (**Figure 20(b)**) which is made to estimate the depth of the source of lava from oceanic domains not influenced by subduction confirms the alkaline nature of the basanite lavas from both sectors and shows that they are located in the garnet stability field. This result suggests that the source of the basanite magma is very deep, located at the level of the enriched lower mantle and would be of the garnet lherzolite type. The existence of garnet in the magmatic source is further confirmed by spectra very depleted in HREE.

4.3.6. Geodynamic Context

The geochemical characteristics of the Quaternary lavas in the Fann and Mermoz sectors are similar to those of the OIBs (oceanic island basalts) (**Figure 20(a)**, **Figure 20(b)**) emplaced by a hot spot. However, the flow in prisms observed of all basanite lavas suggests continental volcanism. This continental volcanism is also confirmed by the geotectonic diagrams of [33] (**Figures 21(a)-(c)**) and [34] (**Figure 21(d)**) which locate the basanite lavas of the two sectors in thedomain of continental intraplate alkaline basalts.

5. Discussion

The Mermoz and Fann sectors, like Mamelles, are emission zones of Quaternary volcanism on the Dakar peninsula. The volcanism of Mermoz had been the subject of detailed study in the past ([6] [19] [35] [36]) contrary to the sector of

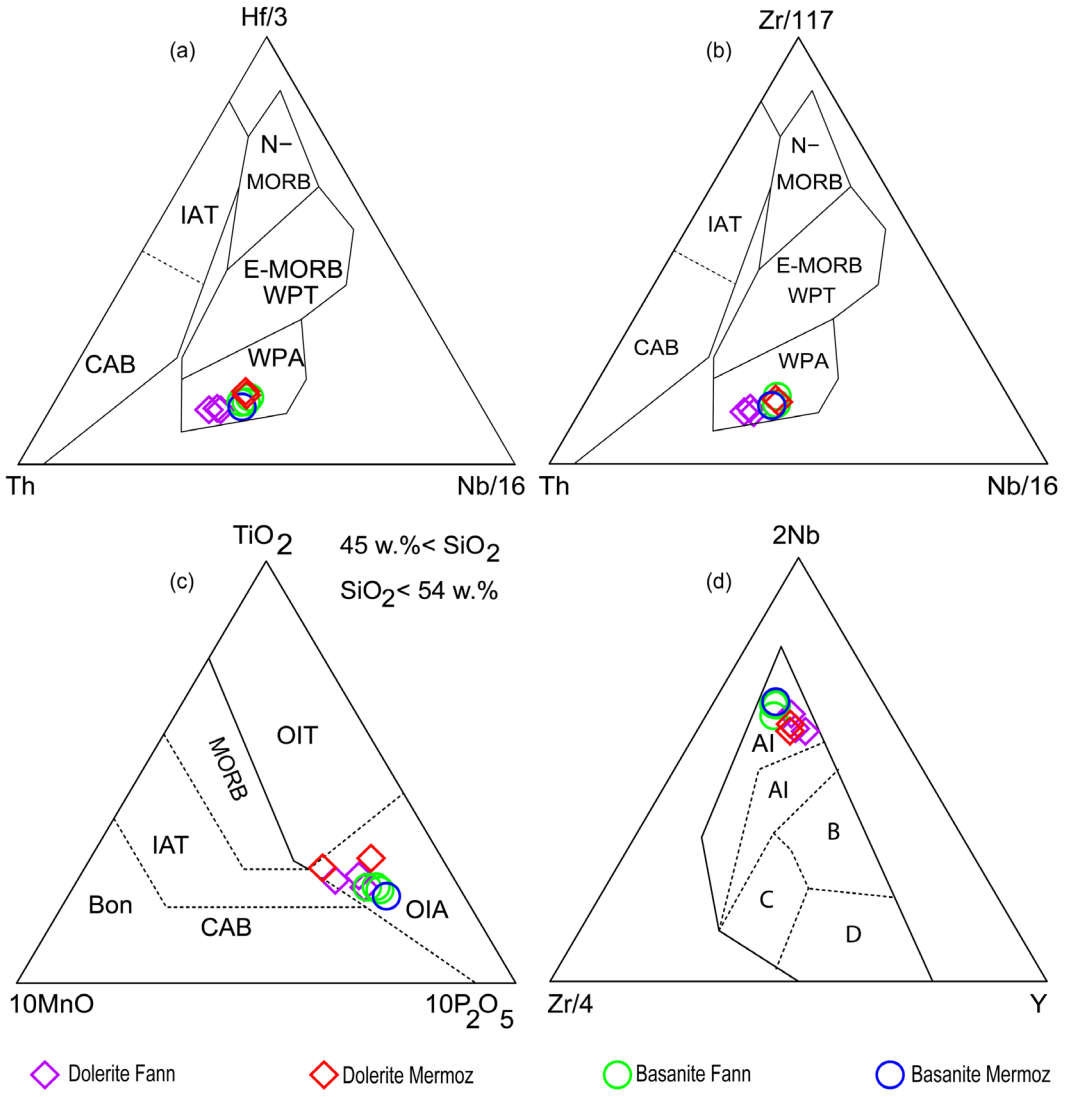

Figure 21. Diagrams of [34] (a)-(c) and [35] (d) showing the geodtynamic context of the magmatic rocks of the Fann and Mermoz sectors.

Fann where only summary works were carried out in particular in certain careers [36]. With regard to Mermoz sector, the lithological succession that we propose is made up from bottom to top: 1) a substratum with at its base Eocene limestones on which lie Quaternary infra-basaltic sands which are themselves surmounted by stratified tuffs from the Mamelles volcano; 2) a ball-shaped vesicular dolerite, with a coarse texture which intersects the previous substratum by deforming the stratified tuffs of the Mamelles volcano. This observation changes the stratigraphic chronology hitherto accepted and which placed the dolerites under the infra-basaltic sands ([16] [17]); 3) a breccia early consisting of slag and dolerite fragments; 4) two generations of basanites that can be cut in prism: the first is vesicular, the second non-vesicular whose placement was guided by vertical fractures oriented N50; 5) a clear intermediate breccia with clayey cement rich in slag, vesicular volcanic bombs and fragments of dolerites;

6) a late breccia with fragments of basanite and dolerite ends the volcanic activity in the Mermoz sector. This breach is mainly located along the NW-SE (N140) and NE-SW (N50) fractures.

The Fann sector contains several emission zones, most of which are currently located in the ocean. The lavas may have reached the coast through E-W and NE-SW faults. The substratum observed in the Mermoz sector is, here, masked by dolerites. There rare outcrops of tuffs interstratified with the dolerites. The new lithological succession that we propose includes from bottom to top: 1) early volcanic breccias; 2) non-vesicular mesocrate D1 dolerite; 3) melanocrate vesicular D2 dolerite; 4) basanites; 5) a late breccia. This succession is very different from those proposed by ([6] [35]) where two generations of dolerites were not distinguished and where the basanites were also placed chronologically under the dolerites ([16] [17] [18] [19]).

Regarding geochemistry, our study confirms the alkaline affinity of the quaternary volcanic rocks suggested by former authors but underlines a heterogeneity of magmatic source for the basanites and the dolerites.

The characteristics of the studied lavas are compatible with a very deep and enriched magmatic source. This is of the garnet lherzolite type located in the lower mantle. The magma would have risen in the form of mantle plumes in favor of the NE-SW and E-W regional faults. This proposal is opposed to that of [19] who had suggested a rise to the surface of material resulting from the partial melting of the upper mantle. On the other hand, it is close to the conclusions issued by [18] based on the Th/Ta and 4He/3He ratios, which locate the source of the quaternary lavas in the lower mantle.

According to the work of [18] the quaternary basanites of Senegal and Cape Verde were set up thanks to the same hot spot located vertically to Cape Verde. However, according to our study, the lavas of Senegal are less enriched in rare earths. The question that arises is: how can lavas from the same source have differences in rare earth compositions? Before examining this question, we will compare the values of the ratios of the highly hygromagmaphilic elements of the basanites of Cape Verde and Senegal. These values are preserved during fractional crystallization processes and partial melting processes: they are therefore characteristics both of the initial liquids and of the mantle sources ([37] [38]). The Th/U, Th/La, La/Ta and Th/Hf ratios (**Table 2**) of the quaternary basanites of Cape Verde and Senegal are very similar. This seems to show that they come from sources of globally identical chemical composition. The greater enrichment in REE of the quaternary lavas of Cape Verde cannot be explained by the classical magmatic processes of the genesis of oceanic basalts. Indeed, the genesis of basalts rich in rare earths by partial melting, at low rates, of a mantle source of the same composition as that at the origin of "normal" basalts, can be excluded [39]. Several fluid-based hypotheses have been proposed to explain the high rare earth contents of basalts around the world. In Hawaii, the abnormal rare earth contents would be the effect of the metasomatic fusion of mineral phases rich in halogens + CO_3 + S + K [40]. At Tahaa (Polynesia), the successive crystallizations

Table 2. Ratio of the hygromagmaphile elements of the basanites of dakar and those of the cape verde islands.

Sector	Dakar								Fogo (Ile de Cap-Vert)					
Lithology	Basanite								Basanite					
Sample	MF161	MF171A	MF175	MF212A	MF200	MF246	MF285	MF266	F-2	F-7	F-8	F-15	F-20	F-24
Th/U	4.53	4.78	4.67	4.16	4.08	3.31	3.33	4.04	4.63	4.85	4.78	4.48	4.27	4.54
Th/La	0.12	0.11	0.11	0.13	0.12	0.11	0.11	0.09	0.1	0.09	0.09	0.09	0.08	0.08
La/Ta	10.17	11.08	11.26	9.10	10.20	7.75	17.96	12.65	6.84	8.77	8.38	7.91	7.77	8.96
Th/Hf	1.14	1.22	1.09	1.25	1.21	1.36	2.30	1.86						

of phosphates with no Ce anomaly, of hydroxides with a positive Ce anomaly, then of carbonates, which would result from the percolation of fluids during an advanced stage of magmatic crystallization, would make it possible to explain the high rare earth contents of basalts [41]. Furthermore, ([42] [43]) proposed for the basalts of Hawaii and those of Polynesia, the hypothesis of a prolonged subaerial alteration accompanied by pedogenesis to explain the enrichment in rare earths of these lavas.

In conclusion, the similarity of the ratios of the hygromagmaphilic elements of the basanites of Cape Verde and Senegal could suggest that these lavas come from a single source. Rare earth enrichment of Cape Verde basanites could be linked to the action of metasomatic fluids as for basalts of Hawaii and Polynesia.

6. Conclusions

The activities of the quaternary magmatism of the Mermoz-Fann zone are associated with tectonic structures having facilitated their establishment.

The substratum of Quaternary volcanism in the Mermoz-Fann zone is made up of: Tertiary marly limestones at the base, covered by Quaternary sands (infra-basaltic sands) which are surmounted by stratified tuffs.

However, it should be noted that this is the first time that the contact between marly limestone and infra-basaltic sands has been highlighted by this study.

In the Mermoz sector, magmatic activity begins with the formation of vesicular dolerite flowing in balls, which deforms the stratified tuffs. This is followed by the emplacement of a scoriaceous breccia. Then, two basanite flows were emplaced in two episodes separated by a period marked by explosions and the emplacement of intermediate breccias.

The Fann sector is largely dominated by the intrusion of two generations of dolerites: the first generation of dolerite (D1) is mesocrate in color and devoid of vesicles, while the second generation of dolerite (D2) is melanocrate and vesicular.

Volcanic activity in the Fann sector is also marked by the establishment of basanite flows with numerous vesicles and vacuoles sometimes filled with carbonates.

Finally, the volcanic activity ends with explosions that affected all the sectors studied. This activity is at the origin of the brecciation of basanites and dolerites.

In addition, the stratified tuffs are the only rocks of the Mamelles volcano intersected by the basanites of Mermoz-Fann. We believe that volcanic products of the Mamelles and those of Mermoz-Fann belong to the same quaternary eruptive system with a main emission zone located at the Mamelles and several

secondary emission zones located between Mermoz and Fann.

From the geochemical point of view, our study confirms the alkaline affinity of the quaternary volcanic rocks of the Dakar region but underlines heterogeneity of magmatic source for basanites and dolerites. These rocks could come from a very deep magmatic source located in the lower mantle. This source is very enriched and of the garnet lherzolite type. The magma from this source would have risen in the form of mantle plumes through major NE-SW and E-W faults in a continental intraplate context.

Acknowledgements

We would like to thank the National Academy of Sciences and Techniques of Senegal (ANSTS) for its financial support for the analytical work. We also thank Mr. Baba Sarr for having authorized and assisted us in the observation of our thin sections at the Fundamental Institute of Black Africa (IFAN).

Conflicts of Interest

The authors declare no conflicts of interest regarding the publication of this paper.

References

[1] Faure, H., Démoulin, D., Hébrard, L. and Nahon, D. (1970) Données sur la néotectonique de l'extrême ouest de l'Afrique. *Conférence de Géologie Africaine Université Ibadan*, *Nigéri*, 609-617.

[2] Bellion, Y. and Crevola, G. (1991) Cretaceous and Cainozoic Magmatism of the Senegal Basin (West Africa): A Review. In: Kampunzu, A.B. and Lubala, R.T., Eds., *Magmatism in Extensional Structural Settings*, Springer, Berlin, 189-208. https://doi.org/10.1007/978-3-642-73966-8_8

[3] Fraudet, P. (1973) Contribution à l'étude des roches éruptives de la région de Thiès (République du Sénégal). *Travaux et Documents des Laboratoires de Géologie de Lyon*, **57**, 15-86.

[4] Hebrard, L. (1974) Découverte de la flore et de la vegetation ensevelies sous les cinérites du volcanisme quaternaire des Mamelles de Dakar (Sénégal). *Bulletin de liaison/Association Sénégalaise pour l'Etude du quaternaire de l'Ouest africaine n*°42-43, 81-90.

[5] Brancart, R.Y. (1975) Etude géologique des feuilles au 1/20000 de la Presqu'île du Cap-Vert, Rufisque-Bargny. Dipl. Etudes sup, Dakar.

[6] Crevola, G. (1974) Les dépôts de déferlantes basales du volcan des Mamelles (Presqu'île du Cap-Vert, Sénégal). *Annales de la Faculté des Sciences*, *Université de Dakar*, **27**, 99-129.

[7] Crevola, G. (1980) Données nouvelles sur le volcanisme quaternaire dans la tête de la Presqu'île du Cap Vert, Sénégal. *Comptes Rendus de l'Académie des Sciences Paris*, *Série D*, **291**, 617-620.

[8] Ligier, J.L. (1980) Structure profonde du basin côtier Sénégalo-mauritanien. Interprétation des données gravimétriques et magnétiques. Thèse 3éme cycle, Trav. Lab. Sci. Terre, Marseille, B, 116, 158 p.

[9] Dia, A. (1980) Contribution à l'étude des matériaux volcaniques de la Presqu'île du

Cap-Vert et du Plateau de Thiès. Inventaire et étude préliminaire des sites. Mém. D.E.A. Fac. Sci. Dakar. Rap. 6nlle série, 90p. 22 fig., 6pl. photo, 10 tab.

[10] Dia, A. (1982) Contribution à l'étude des caractéristiques pétrographiques, pétrochimiques et géotechniques des granulats basaltiques: de la Presqu'île du Cap-Vert et du Plateau de Thiès, carrière de Diack, Sénégal. Master's Thesis, Université de Dakar, Dakar.

[11] Sustrac, G. (1984) Plan minéral de la république du Sénégal. Rapport du B.R.G.M (Bureau de Recherches Géologiques et Minières).

[12] Lompo, M. (1987) Méthodes et étude de la fracturation et des filons; exemple de la région du Cap-Vert (Sénégal). Mém. D.E.A. Fac. Sci. Dakar., 59 p, 16 fig., 2 ann.

[13] Lo, P.G. (1988) Le volcanisme quaternaire de Dakar (Sénégal Occidental): Particularités pétrographiques, caractères géochimiques, implications pétrogénétiques. Thèse 3è cycle, Nancy-Université, Lorraine, 202 p.

[14] Lo, P.G., Dia, A. and Kampunyu, A.B. (1992) Cenozoic Volcanism in Western Senegal and Its Relationship to the Opening of the Central Atlantic Ocean. *Tectonophysics*, **209**, 281-291. https://doi.org/10.1016/0040-1951(92)90035-5

[15] Mellet, O. (1993) Etude des mécanismes de mise en place et de la pétrogenèse du volcano-sédimentaire quaternaire de la Presqu'île du Cap-Vert (Sénégal occidental). Mem. DEA Geosciences, INPL, Nancy.

[16] Crevola, G., Cantagrel, J.M. and Moreau, C. (1994) Le volcanisme cénozoïque de la Presqu'île du Cap-Vert (Sénégal); cadre chronologique et géodynamique. *Bulletin de la Société géologique de France*, **165**, 437-446.

[17] Ndiaye, A. (2002) Etude lithologique et pétrographique des coulées de laves quaternaires de la Presqu'île du Cap-Vert (Sénégal). Mém. DEA Fac., Sciences et Techniques Univ. Ch. A. DIOP, Dakar.

[18] Yatte, D. (2017) Etude géochimique comparative entre les laves tertiaires et quaternaires du Sénégal occidental et celles des îles du Cap-Vert, apport du traceur hélium: Implications géodynamiques. Master's Thesis, Université Cheikh Anta Diop de Dakar, Dakar.

[19] Lo, P.G. (2002) Le volcanisme quaternaire de la Presqu'île de Dakar (Sénégal Occidental); relations chronologiques entre deux appareils, en système distensif; implications pétrogénétiques. *Garcia de Orta, Serie de Geologia*, **18**, 19-33.

[20] Tessier, F. (1952) Contributions à la stratigraphie et à la paléontologie de la partie ouest du Sénégal (Crétacé et Tertiaire). Grande Imprimerie africaine, Dakar.

[21] Bellion, Y. and Guiraud, R. (1984) Le basin sédimentaire du Sénégal. Synthèse des connaissances actuelles. In: Bureau des Recherches Geologiques et Minieres (BRGM) et Direction des Mines et de la Geologie (DMG), Dakar, Eds., *Plan Mineral de la Republique du Senegal*, Bureau des Recherches Geologiques et Minieres (BRGM) et Direction des Mines et de la Geologie (DMG), Dakar, 4-63.

[22] Crevola, G. (1978) Sills, dykes, et pipes de tufs volcaniques bréchiques fluidifiés dans la Presqu'île du Cap-Vert (Sénégal). *Comptes Rendus Sommaires de la Société Géologique de France*, **3**, 135-139.

[23] Barusseau, J.P. and Gaye, C. (1983) Sur l'origine et l'âge des sables situés sous les formations du volcanisme quaternaire de la Presqu'île du Cap-Vert (Sénégal) (sables infrabasaltiques). *Bulletin de liaison-Association Sénégalaise pour l'étude du quaternaire de l'ouest africain*, **70-71**, 43-52.

[24] Barrat, J.A., Zanda, B., Jambon, A. and Bollinger, C. (2014) The Lithophile Trace Elements in Enstatite Chondrites. *Geochimica and Cosmochimica Acta*, **128**, 71-94. https://doi.org/10.1016/j.gca.2013.11.042

[25] Sun, S.S. and McDonough, W.F. (1989) Chemical and Isotopic Systematics of Oceanic Basalts: Implications for Mantle Compositions and Processes. *Geological Society*, *London*, *Special Publications*, **42**, 313-345. https://doi.org/10.1144/GSL.SP.1989.042.01.19

[26] Yatte, D., Diallo, D.P. and Sagna, I. (2015) Comparative Geochemical Study of the Tertiary and Quaternary Lavas of Western Senegal and the Cape Verde Islands: Geodynamic Implications. *International Journal of Geosciences*, **6**, 1193-1213. https://doi.org/10.4236/ijg.2015.611094

[27] Doucelance, R., Escrig, S., Moreira, M., Gariépy, C. and Kurz, M.D. (2003) Pb-Sr-He Isotope and Trace Element Geochemistry of the Cape Verde Archipelago. *Geochimica and Cosmochimica Acta*, **67**, 3717-3733. https://doi.org/10.1016/S0016-7037(03)00161-3

[28] Smietana, M. (2011) Pétrologie, géochronologie (K-Ar) et géochimie élémentaire et isotopique (Sr, Nd, Hf, Pb) de laves anciennes de La Réunion: Implications sur la construction de l'édifice volcanique. Thèse de Doctorat, Université de La Réunion, Saint-Denis.

[29] Winchester, J.A. and Floyd, P.A. (1977) Geochemical Discrimination of Different Magma Series and Their Differentiation Products Using Immobile Elements. *Chemical Geology*, **20**, 325-343. https://doi.org/10.1016/0009-2541(77)90057-2

[30] Pearce, J.A. (1996) A User's Guide to Basalt Discrimination Diagrams. Trace Element Geochemistry of Volcanic Rocks: Applications for Massive Sulphide Exploration. *Geological Association of Canada*, *Short Course Notes*, **12**, 79-113.

[31] Pouclet, A., Vidal, M., Delor, C., Simeon, Y. and Alric, G. (1996) Le volcanisme birimien du nord-est de la Cote-d'Ivoire, mise en évidence de deux phases volcano-tectoniques distinctes dans l'évolution géodynamique du Paleoproterozoique. *Bulletin de la Société géologique de France*, **167**, 529-541.

[32] Pearce, J.A. (2008) Geochemical Fingerprinting of Oceanic Basalts with Applications to Ophiolite Classification and the Search for Archean Oceanic Crust. *Lithos*, **100**, 14-48. https://doi.org/10.1016/j.lithos.2007.06.016

[33] Wood, D.A. (1980) The Application of a Th-Hf-Ta Diagram to Problems of teCtonomagmatic Classification and to Establishing the Nature of Crustal Contamination of Basaltic Lavas of the British Tertiary Volcanic Province. *Earth and Planetary Science Letters*, **50,** 11-30. https://doi.org/10.1016/0012-821X(80)90116-8

[34] Meschede, M. (1986) A Method of Discriminating between Different Types of Mid-Ocean Ridge Basalts and Continental Tholeiites with the Nb 1bZr 1bY Diagram. *Chemical Geology*, **56**, 207-218. https://doi.org/10.1016/0009-2541(86)90004-5

[35] Debant, P. (1963) Les roches volcaniques récentes de la feuille au 1: 20000è de Ouakam (République du Sénégal). *Annales de la Faculté des sciences*, *Université de Dakar*, **10**, 79-154.

[36] Crevola, G. (1975) Le volcanisme tertiaire et quaternaire de la presqu'île du Cap-Vert (Sénégal). *Bulletin de l'Association pour l'Avancement des Sciences Naturelles au Sénégal* (*AASNS*), **40**, 19-39.

[37] Treuil, M. and Varet, J. (1973) Critères volcanologiques, pétrologiques et géochimiques de la genèse et de la différenciation des magmas basaltiques, exemple de l'Afar. *Bulletin de la Société Géologique de France*, **S7-XV**, 401-644. https://doi.org/10.2113/gssgfbull.S7-XV.5-6.506

[38] Treuil, M. and Joron, J.L. (1975) Utilisation des elements hygromagmaphiles pour la simplification de la modélisation quantitative des processus magmatiques. Exemples

de l'Afar et de la dorsal médio-atlantique. *Societa Italiana Mineralogia e Petrologia—Milano*, **XXXI**, 125-174.

[39] Déruelle, B., Figueroa, O.A., Joron, J.L., Schilling, M., Silva, C. and Herve, F. (2002) Le volcanisme de l'île de Pâques (Chili). *Géologie de la France*, **2**, 53-67.

[40] Fodor, R.V., Bauer, G.R., Jacobs, R.S. and Bornhorst, T.J. (1987) Kahoolawe Island, Hawaii: Tholeiitic, Alkalic, and Unusual Hydrothermal (?) "Enrichment" Characteristics. *Journal of Volcanology and Geothermal Research*, **31**, 171-176. https://doi.org/10.1016/0377-0273(87)90015-1

[41] Joron, J.L., Schiano, P., Turpin, L., Treuil, M., Gisbert, T., Leotot, C. and Brousse, R. (1991) Exceptional Rares Earth Elements Enrichments in Tahaa Volcano (French Polynesia). *Comptes Rendus de l'Académie des Sciences*, *Série II*, **313**, 523-530.

[42] Fodor, R.V., Frey, F.A., Bauer, G.R. and Clague, D.A. (1992) Ages, Rare-Earth Element Enrichment, and Petrogenesis of Tholeiitic and Alkalic Basalts from Kahoolawe Island, Hawaii. *Contributions to Mineralogy and Petrology*, **110**, 442-462. https://doi.org/10.1007/BF00344080

[43] Cotten, J., Le Dez, A., Bau, M., Caroff, M., Maury, R.C., Dulski, P. and Brousse, R. (1995) Origin of Anomalous Rare-Earth Element and Yttrium Enrichments in Subaerially Exposed Basalts: Evidence from French Polynesia. *Chemical Geology*, **119**, 115-138. https://doi.org/10.1016/0009-2541(94)00102-E